EUROPEAN RESPIRATORY *journal*

FLAGSHIP SCIENTIFIC JOURNAL OF ERS

Early View

Original article

The NLRP3 inflammasome pathway is activated in sarcoidosis and involved in granuloma formation

Christine Huppertz, Benedikt Jäger, Grazyna Wieczorek, Peggy Engelhard, Stephen J. Oliver, Franz-Georg Bauernfeind, Amanda Littlewood-Evans, Tobias Welte, Veit Hornung, Antje Prasse

Please cite this article as: Huppertz C, Jäger B, Wieczorek G, *et al*. The NLRP3 inflammasome pathway is activated in sarcoidosis and involved in granuloma formation. *Eur Respir J* 2020; in press (https://doi.org/10.1183/13993003.00119-2019).

The NLRP3 inflammasome pathway is activated in sarcoidosis and involved in granuloma formation

Christine Huppertz,[1†] Benedikt Jäger,[2,3,4†] Grazyna Wieczorek,[1] Peggy Engelhard,[3,4] Stephen J. Oliver,[1] Franz-Georg Bauernfeind,[5] Amanda Littlewood-Evans,[1] Tobias Welte,[7,8] Veit Hornung,[6] Antje Prasse,[2,4,7,8*]

[1] Department of Autoimmunity, Transplantation and Inflammation, Novartis Institutes for BioMedical Research, Basel, Switzerland
[2] Fraunhofer ITEM, Hannover, Germany
[3] Faculty of Biology, Albert Ludwig University Freiburg, Germany
[4] Department of Pneumology, University Medical Center Freiburg, Germany
[5] Department of Internal Medicine III, University Hospital Bonn, Bonn, Germany
[6] Gene Center and Department of Biochemistry, Ludwig-Maximilians-Universität München, Munich, Germany
[7] Department of Pulmonology, Medical School Hannover, Germany
[8] DZL, BREATH, Hannover, Germany

† both authors contributed equally

*** corresponding author:**

Antje Prasse, Hannover Medical School, Carl-Neuberg-Strasse 1, 30625 Hannover, Germany,
Tel. ++49 511 532 3531; FAX ++49 511532 3353
E-Mail: prasse.antje@mh-hannover.de

ABSTRACT

Sarcoidosis is a disease characterized by granuloma formation. There is an unmet need for new treatment strategies beyond corticosteroids. The NLRP3 inflammasome pathway is expressed in innate immune cells and senses danger signals to elicit inflammatory IL-1β and recently has become a druggable target. This prompted us to test the role of the NLRP3 inflammasome and IL-1β pathway in granuloma formation and sarcoidosis.

Nineteen sarcoid patients and 19 healthy volunteers (HV) were recruited into this pilot study. NLRP3 inflammasome activity was measured in BAL-cells and lung and skin biopsies using immunohistochemistry, Western blot, RT-PCR and ELISA. For in vivo experiments we used the trehalose 6,6 dimycolate (TDM)- granuloma mouse model and evaluated lung granuloma burden in miR-223 KO and NLRP3 KO mice as well as the treatment effects of MCC950 and anti-IL-1β antibody therapy.

We found strong upregulation of the NLRP3 inflammasome pathway, evidenced by expression of activated NLRP3 inflammasome components, including cleaved caspase-1 and IL-1β in lung granuloma, and increased IL-1β release of BAL-cells from sarcoid patients compared to HV ($p=0.006$). mRNA levels of miR-223, a micro RNA downregulating NLRP3, were decreased and NLRP3 mRNA correspondingly increased in alveolar macrophages from sarcoid patients ($p<0.005$). NLRP3 KO mice showed decreased and miR-223 KO mice increased granuloma formation compared to wildtype. Pharmacological interference using NLRP3 pathway inhibitor MCC950 or an anti-IL-1β antibody resulted in reduced granuloma formation ($p<0.02$).

In conclusion, our data provide evidence of upregulated inflammasome and IL-1β pathway activation in sarcoidosis and suggest both as valid therapeutic targets. .

NOTES

Author contributions

Conception and design: C.H., B.J., G.W., S.J.O., F.G.B., V.H. and A.P.. Experiments with human materials and analyses: C.H., B.J., G.W., S.J.O., F.B., and A.P.. Experiments with mice and murine materials and analyses: C.H., P.E., B.J., G.W., F.G.B. and A.P.. Manuscript preparation: C.H., B.J., G.W, S.J.O., P.E., A.L.E, F.G.B., V.H., and A.P.

Acknowledgments

We would like to thank Victoria Wirtz, Marija Curcic, Antje Marcantonio as well as Gaelle Elain for expert technical assistance.

Funding

Part of this work was funded by a research grant from Novartis to the University Medical Center Freiburg (PI: A.P.). Further funding was provided by DZL BREATH.

Competing Interests

A.P. was a consultant to Novartis, Sanofi-Aventis, and Bayer and currently consults for Boehringer Ingelheim, Roche and Nitto. A.P. is a recipient of research grants from Novartis in the past and presently Boehringer Ingelheim, AstraZeneca and AdAlta. A.P. received speaker honorium from Boehringer Ingelheim, Novartis, AstraZeneca, and Roche.
C.H., G.W., S.J.O. and A.L.E. are employees of Novartis Pharma AG. These authors have no additional financial interests.
All other authors declare no competing financial interests.

Abbreviation list

BAL bronchoalveolar lavage, HV healthy volunteer, SAA serum amyloid A, PBMC peripheral blood mononuclear cells, TBB transbronchial biopsies, TDM trehalose 6,6-dimycol

INTRODUCTION

Sarcoidosis is a systemic disease characterized by non-necrotizing granuloma formation in genetically susceptible individuals [1-4]. The exact causative trigger factor is still unknown and there are likely to be various triggers [1, 5]. Recent findings suggest that pathogen associated molecular patterns (PAMPs) derived from mycobacteria or propionibacteria may trigger an exaggerated immune response in sarcoid patients [5, 6]. It is thought that a misled host response to otherwise harmless PAMPs amplifies the immune response in sarcoidosis [3]. The group of Moller and colleagues showed that serum amyloid A (SAA) was highly expressed by sarcoid granuloma [7]. If needed, patients are treated with immunosuppressants, often for years or even decades. Longterm steroid treatment use for patients with sarcoidosis often results in increased burden of co-morbid side effects and new treatment concepts are urgently warranted [1, 2, 8, 9].

Over the past 3 decades there have been multiple studies to suggest that macrophages from sarcoidosis produce a broad spectrum of M1 cytokines that include TNF-α, CXCL10 and IL-1β [10-17]. Several reports have indicated a pathogenic role for IL-1β in sarcoidosis [11-16, 18-20] almost 30 years ago.However, the IL-1β family has recently regained tremendous interest due to the molecular delination of the so called inflammasome pathway, an intracellular multiprotein complex that plays a crucial role in the production and release of biologically active IL-1β by macrophages [17, 21]. The most studied inflammasome is the NLRP3 inflammasome which was found to be critically involved in the pathogenesis of several diseases including silicosis, tuberculosis and Alzheimer`s disease [22-24]. Among others, silicate crystals as well as amyloid fibrils can activate the NLRP3 inflammasome [25-28]. NLRP3 inflammasome assembly requires two signals, a priming signal which results in the transcription of pro-IL-1β and NLRP3, and a second signal that promotes indirect activation of the inflammasome by factors such as ATP or nigericin [17, 21]. NLRP3 inflammasome oligomerization leads to the activation of caspase-1 and expression of the functionally active caspase-1 p10 and p20 subunits [17]. Activated caspase-1 subsequently cleaves pro-IL-1β into the biologically active form of IL-1β. Based on these new insights in inflammasome and IL-1β immunobiology, several new treatment strategies blocking the NLRP3 inflammasome and IL-1β signaling have been developed and even approved for certain diseases [29].

On the background of these findings we became interested in the role of the NLRP3 inflammasome in sarcoidosis. We observed that this inflammasome pathway is indeed active in

human samples of sarcoidosis patients compared to healthy volunteers. Further, using a mouse model of pulmonary granuloma formation, we could determine the significance of IL-1β and inflammasome components contributing to the pathology of sarcoidosis.

METHODS

Study population

This study enrolled 19 patients with sarcoidosis (SARC), 6 patients with interstitial lung disease in the context of scleroderma (SSc) and 19 healthy volunteers (HV; Table 1). The study was conducted at the University Medical Center Freiburg, Germany and was approved by the local ethics committee. All subjects provided written informed consent before participating in the study. In 18 of the 19 sarcoid patients bronchoscopy was performed within the routine diagnostic work-up at initial diagnosis. Sarcoid disease activity of the lung was defined as 'mild' for inactive lung disease with normal pulmonary function and no respiratory symptoms, 'moderate' for active lung disease with no requirement for immunosuppressive (IS) treatment according to the guidelines proposed by the American Thoracic Society/European Respiratory Society [30], or 'severe' for active lung disease with the requirement for IS treatment. These patients categorized with 'severe' disease activity with need for IS treatment had severe lung parenchymal (>20%) involvement and an inflammatory phenotype (e.g. elevated levels of sIL-2R and BAL lymphocytosis). We did not recruit patients with advanced, non-inflammatory, fibrotic disease into this study. All included patients classified as suffering from severe disease underwent bronchoscopy and BAL during the routine diagnostic work-up at initial diagnosis.

Bronchoalveolar lavage, transbronchial biopsies

Bronchoalveolar lavage (BAL), transbronchial and skin biopsies were performed in sarcoidosis patients as part of their routine diagnostic work-up in accordance to a standardized protocol [31-33]. For further details see supplement.

Histopathology and immunohistochemistry of human biopsies

Paraffin tissue sections from human transbronchial biopsies or skin biopsies were stained with hematoxylin and eosin (H&E) and immunohistochemically, using primary antibodies specific for various markers. For further details see supplement.

Immunoblot analysis of caspase-1p20 activity

BAL cells were stimulated w/wo the NLRP3 activation protocol described in detail in the supplement and supernatants were precipitated with methanol/chloroform. Cleaved caspase-1 (p20) was detected in the supernatants using primary antibody rabbit mAb cleaved caspase-1 (Cell Signalling Technology).

MicroRNA analysis and RT-PCR

Alveolar macrophages were sorted from BAL cells from sarcoid patients and healthy volunteers on a MoFlo Astrios/Beckman Coulter cell sorter based on cell characteristics in the forward/sideward scatter and typical autofluorescence of AMs. Total cellular miRNA from 10^6 sorted AMs was isolated using mirVana™ isolation kit (Thermo Fisher Scientific). Further details are given in the supplement.

Animal studies

NLRP3 -/- mice (B6 strain background) were kindly provided by Dr. Dixit from Genentech. MiR-223 -/- mice (B6.Cg-Ptprca Mir223tm1Fcam/J), their respective wildtype (B6.SJL-Ptprc^a Pepc^b/BoyJ) control mice and C57BL/6J wildtype (WT) mice were purchased from the Jackson Laboratory/USA. For further details see supplement.

Murine pulmonary granuloma model induced by trehalose 6,6'-dimycolate (TDM)

TDM (Enzo Life Sciences GmbH, Germany, catalog#: ALX-581-210-M001) from mycobacterium tuberculosis was prepared in a water in oil emulsion using incomplete Freund`s Adjuvant as described [34, 35] and injected into tail vein. To assess pulmonary granuloma formation, lungs were harvested on day 7 after TDM injection for all studies. In addition WT mice were administered vehicle (PBS) or MCC950, a NLRP3 inflammasome pathway inhibitor, at 10 mg/kg intraperitoneally on day 0, 1, 2, 4, and 6 after TDM injection. In another experiment WT mice were administered subcutaneously with either vehicle (PBS), isotype control antibody anti-cyclosporine (Novartis) [200µg/mouse] or anti-IL-1β antibody (Novartis) [200µg/mouse] on day -1 and again 3 days after TDM injection. For further details see supplement.

RESULTS

Study cohort

Clinical characteristics and BAL differentials are given in Table 1. Of the 19 patients with sarcoidosis, 11 had severe lung disease activity with significantly decreased lung function and requirement for immunosuppressive treatment because of lung involvement, 3 had moderate and 5 had mild lung disease activity (Table 1). None of the patients classified as moderate or mild were in need for immunosuppressive treatment because of lung involvement. All 6 scleroderma patients had significant lung disease and underwent bronchoscopy because of respiratory deteroriation and need for immunosuppressive treatment. All of the study participants were non-smokers. All subjects were of Caucasian ethnicity except for one African-American. All sarcoid patients were treatment-naïve except one patient with severe disease who received low dose prednisone (5 mg/d). As expected, BAL of sarcoid patients contained increased total cell counts and a significantly higher proportion of lymphocytes compared to BAL from HVs, while percentage of alveolar macrophages (AM) was reduced (Table 1). The mean age of all sarcoid patients was significantly increased compared to the mean age of HV ($p< 0.0001$), while the age across the patients grouped by pulmonary disease activity did not differ significantly. Importantly, there was no statistically significant effect of age on all outcomes described below.

Evidence of inflammasome activation and IL-1β expression in sarcoid granulomas

Sarcoid granulomas were composed of CD68-positive macrophages (Fig. 1A, B). Expression of active caspase-1 depicted with an antibody against cleaved/active caspase-1 (for characterization see Suppl. Fig. S1) was shown in areas that corresponded to CD68-positive granulomas frequently containing multinucleated giant cells (Fig. 1D, E). This pattern was observed in almost all cases of transbronchial and skin biopsies (Fig. 1 A-F, Fig. S2, S3). Immunoreactivity for IL-1β was observed within the granulomas in all biopsies (Fig. 1G, H; Fig. S2, S3). Sarcoid granulomas were thus composed primarily of CD68-positive macrophages which stained positively for active caspase-1 and IL-1β. For IL-1β staining, a blinded, semi-quantitative scoring by an expert pathologist was performed and revealed a trend for higher IL-1β expression in lung granulomas from patients with severe lung disease compared with patients with milder disease ($n=13$, $p= 0.1111$, Fig. 1L).

Evidence for an activated NRLP3 inflammasome pathway in BAL cells and monocytes derived from sarcoid patients

The constitutive release of IL-1ß from sarcoid BAL cells was significantly increased compared to levels determined for BAL cells from HV (p= 0.0065, Fig. 2A) or scleroderma patients (p=0.038, Fig.2A). Furthermore, BAL cells from the sarcoid patients with severe disease showed significantly increased constitutive IL-1ß production compared with HV (p= 0.0161, Fig. 2B). Compared to constitutive IL-1ß release, upon *ex-vivo* stimulation of the NLRP3 inflammasome with LPS/nigericin, there was at least a ten-fold increase in IL-1ß production from BAL cells derived from HV and from sarcoid patients (Fig. 2A and C). BAL cells obtained from sarcoidosis patients elicited significantly more IL-1ß compared to those from HV upon NLRP3 inflammasome stimulation (p< 0.0001, Fig. 2C), and this ability increased with the activity of lung disease (mild versus severe disease activity, p= 0.0020, Fig. 2D). Similar findings were obtained upon NLRP3 inflammasome stimulation with LPS/ATP (Fig. 2D). Western blot analysis confirmed active IL-1β production by BAL cells (Fig. S4). Expression and activation state of the caspase-1 enzyme was studied in BAL cells from HV and sarcoid patients by Western blot. We found increased constitutive expression of the activated caspase-1 p20 in the conditioned medium of unstimulated BAL cells from sarcoid patients compared to BAL cells from HV (Fig. 2E). Levels of activated caspase-1 p20 were enhanced in conditioned medium of LPS/Nigericin- or LPS/ATP-stimulated BAL cells, again with BAL cells derived from sarcoid patients containing higher levels than HV samples (Fig. 2E).

In the same cohort we also studied inflammasome activation of monocytes isolated from peripheral blood. Of note, the NLRP3 inflammasome and IL-1β release is differently activated and regulated in monocytes compared to macrophages. Monocytes from sarcoid patients showed an increased release in IL-1β following LPS stimulation in contrast to monocytes from HV (p=0.0069, FigS5).

Since miR-223 has been shown previously to downregulate NLRP3 transcription in mouse bone-marrow derived cells by our group [36], we studied the RNA expression of miR-223 and NLRP3 in FACS-sorted alveolar macrophages by RT-PCR. We found a significant decrease in relative miR-223 expression (p= 0.0002, Fig. 2F) and a significant increase in relative NLRP3 expression (p= 0.0023, Fig. 2G) in sorted alveolar macrophages from sarcoid patients compared

to HV. Thus, reduced miR-223 levels likely contribute to increased NLRP3 expression and NLRP3 inflammasome pathway activation in sarcoidosis.

Downstream effects of IL-1ß signaling are upregulated in sarcoid patient samples

Because of the increased IL-1ß levels observed in sarcoid patients, we became interested in downstream effects of IL-1ß signaling and investigated the expression of IL-1 receptor antagonist (IL-1ra) and IL-8, both of which are inducible by IL-1β. Constitutive levels of IL-1ra released from BAL cells cultured *ex vivo* for 24h were highly elevated for sarcoid patients compared to HV (p= 0.0038, Fig. 3A) and increased with disease activity (p= 0.0001, Fig. 3B). The levels of the neutrophil chemoattractant IL-8 released by BAL cells were also increased in sarcoidosis (p= 0.0074 and p= 0.0004, Fig. 3C and D). We found a statistically significant correlation between IL-1ra and IL-8 levels (r^2= 0.860, p<0.0001, Fig. S6) and between constitutive IL-1β and IL-8 production (r^2= 0.559, p=0.0006, Fig. S6). Neutrophils comprised only a low fraction of the overall BAL cell populations recovered from both sarcoid patients and HVs as expected. However, neutrophil counts when normalized per total cell counts/100 ml BAL fluid were increased in sarcoid patients compared to HV (p= 0.0256), and were especially significantly increased in patients with severe compared to mild disease (p= 0.0018, Table 1). Furthermore, blood neutrophil counts in sarcoid patients with severe lung disease activity were also significantly elevated compared to HV (p= 0.0458, Fig. 3E).

Upregulated SAA levels in sarcoid patients perpetuate NLRP3 inflammasome activity

As SAA has been proposed as a main driver in the pathogenesis of sarcoidosis and also as an activator of the NLRP3 inflammasome [7], we analyzed the expression and effects of SAA in the context of the NLRP3 inflammasome pathway; the details of these analyses are provided in the supplement (Fig S7).

The NLRP3 inflammasome pathway is active in a mouse model of granuloma formation

The glyocolipid trehalose 6,6-dimycolate (TDM) when injected intravenously induces pulmonary granuloma in mice. Representative photomicrographs of pulmonary granuloma induced by TDM in wildtype (WT) mice are shown in Fig. 4A-C, Fig. S8 and Fig. S9. Total granuloma burden of the left lobe of the lung was counted and exemplified in Fig. 4B. We investigated the functional responsiveness of the murine BAL cells to NLRP3 inflammasome

stimulation by LPS/nigericin (and LPS/ATP). We found increased IL-1β release from the TDM-treated versus untreated mice ($p= 0.0006$, Fig. 4D), reflecting an increased inflammasome activation in this model. Consecutive immunohistochemically stained sections revealed an accumulation of Iba-1-positive macrophages (Fig. 4E,F, Fig. S8 and Fig. S9) and expression of IL-1β in the granuloma corresponding to the same area (Fig. 4G, Fig. S9). Furthermore we could show SAA staining in the TDM-induced granulomas (Fig. 4H, Fig. S9). To address the impact of the NLRP3 inflammasome and miR-223 on granuloma formation, we analyzed the effects of genetic ablation of these molecules in the TDM model. We found significantly increased granuloma counts in lungs from miR-223 -/- mice ($p= 0.0016$) and reduced granuloma counts in lungs from NLRP3-/- mice ($p< 0.0001$) compared to WT (Fig. 4I-L). Moreover, in miR-223 KO mice we observed larger and more confluencing granuloma than in wildtype or NLRP-/-mice.

To assess the effects of pharmacological intervention of the NLRP3 inflammasome pathway, the NLRP3 inflammasome pathway inhibitor MCC950 was administered for 7 days to the TDM-treated WT mice, resulting in a significant reduction of pulmonary granuloma formation ($p= 0.002$, Fig. 4M-N). Similarly, treatment with anti-IL-1β antibodies significantly reduced granuloma counts compared to vehicle control ($p= 0.0184$, Fig. 4O-P) and isotype control antibody ($p= 0.021$, Fig. 4P).

DISCUSSION

Sarcoidosis is a granulomatous disease with a high unmet medical need which urgently requires new treatment strategies. In our paper we demonstrate the significance of the inflammasome as a key factor in sarcoidosis development and disease severity and identify this pathway as a potential treatment target for sarcoidosis. We show that inflammsome components and active IL-1β are expressed by macrophages and multinucleated giant cells within the sarcoid granuloma. Furthermore, in contrast to healthy volunteers, the NLRP3 inflammasome is constitutively activated in alveolar macrophages from patients with sarcoidosis and levels of NLRP3 inflammasome activation correlate with disease activity. These results clearly demonstrate that NLRP3 inflammasome activation takes place within the granuloma and appears to be initiated by signals present in the lesion. Furthermore, we provide supportive preclinical data in an experimental model of sarcoidosis in which granuloma formation is induced by the mycobacterial derived glycolipid TDM, to demonstrate the amplifying role of NLRP3 inflammasome activation in pulmonary granuloma formation.

Immunohistochemistry revealed that both active caspase-1 and IL-1β protein are highly expressed by multinucleated giant cells within the sarcoid granuloma as well as by sarcoid tissue macrophages, but not in normal lung and skin. BAL cells from patients with sarcoidosis spontaneously released both IL-1β and the active subunit of caspase-1 in contrast to cells derived from healthy volunteers or scleroderma patients. Moreover, a stimulation protocol resulting in NLRP3 inflammasome activation demonstrated NLRP3 inflammasome hyperactivation in sarcoid BAL cells compared to healthy cells. Recent findings highlight the crucial role of inflammasomes as sensors of pathogens and danger signals [14-16]; the body needs to differentiate between harmless and deleterious PAMPs and DAMPs, and inflammasomes help direct the innate immune responses and maintain lung tissue homoeostasis. Thus under normal conditions, inflammasome activation and IL-1β production are tightly regulated because of their potentially deleterious effects [17, 21]. In our sarcoid patient cohort however, we found dysregulated NLRP3 inflammasome activation and consecutive IL-1β release highly increased in patients with severe disease and need for immunosuppressive treatment. Almost 30 years ago researchers noted a correlation of BAL fluid IL-1β levels with disease activity [13, 14], increased IL-1β gene expression of sarcoid alveolar macrophages and increased IL-1ra levels [20, 37, 38]

which we now attribute to enhanced inflammasome activity in this study. Of note, in familial sarcoidosis, the Blau syndrome, a mutation in the Nod2 gene causing activation of NFκb via an alternative NLR pathway was described [39, 40]. Moreover, in our sarcoid cohort, increased IL-1β release was associated with downstream IL-1R1 signaling events such as elevated IL-1ra and IL-8 levels and ensuing neutrophil influx. Higher BAL neutrophil counts were reported in more severly affected patients with need for immunosuppressive treatment. [41, 42]. Increased IL-1β production by antigen presenting cells such as macrophages and increased IL-1R signaling drives also generation of TH17.1 cells which were recently found to be increased in sarcoidosis and may act as a key pathogenetic element [43-45]. Thus, our findings demonstrate that constitutive NLRP3 inflammasome activation in sarcoidosis appears to be of both pathophysiologic and clinical relevance.

Recent immunohistopathological analysis shows accumulation of the acute phase protein SAA in the center of the sarcoid granuloma in close proximity to multinucleated giant cells [7, 46]. Indeed by its distribution and proximity to macrophages and correlation with $CD3^+$ cell influx, the authors claim that SAA coordinates innate and adaptive immune responses to aid development of granulomatous inflammation in sarcoidosis and potentially other granulomatous diseases. Further, the authors use a murine experimental model of sarcoidosis to substantiate their theory that SAA contributes to development of granulomas. Others suggest NLRP3 inflammasome activation by SAA in human and mouse macrophages in vitro, in human psoriatic keratinocytes ex vivo and preclinically in murine asthma models [25-27]. We observed that in line with previously published data, serum SAA levels were increased in our cohort of sarcoid patients [47, 48]. Following stimulation with SAA, BAL-cells from patients with sarcoidosis released IL-1β in contrast to cells derived from healthy volunteers. Furthermore, SAA-induced IL-1β production by peripheral blood monocytes was efficiently blocked by the caspase-1 inhibitor VX-740 and the NLRP3 inflammasome inhibitor MCC950. In the light of a previous publication [7], our data suggest that SAA may be a potential endogenous DAMP capable of triggering NLRP3 inflammasome activation in sarcoidosis. To substantiate this we also found accumulation of SAA in the granulomatous lesions in our murine model, where mycobacterial-derived TDM evokes pulmonary granuloma. Further, TDM-induced granuloma formation was markedly attenuated in NLRP3-/- mice compared to wildtype animals.

One additional mechanism by which NLRP3 inflammasome activation is regulated is through miR-223, which directly targets NLRP3 expression levels [36, 49, 50]. In comparison to alveolar macrophages from healthy volunteers, miR-223 expression levels of sarcoid alveolar macrophages were significantly reduced, while NLRP3 expression was significantly upregulated. Since NLRP3 expression levels are closely correlated with NLRP3 inflammasome activity, our findings suggest that reduced miR-223 expression of sarcoid macrophages may contribute to the constitutive activation of the NLRP3 inflammasome. Since miR-223-deficient mice showed an increase in NLRP3 inflammasome activity and granuloma formation compared to the respective wildtype animals in the sarcoidosis model in vivo, this assumption is reinforced. Thus, our data suggest a pivotal role of the NLRP3 inflammasome and miR-223 depletion in amplifying granuloma formation.

We used the same TDM granuloma model to test therapeutic strategies which interfere with NLRP3 inflammasome activation and IL-1β signaling. MCC950 is a recently developed small molecule inhibiting NLRP3 inflammasome assembly and activation [29]. Mice treated with MCC950 showed significantly reduced lung granuloma burden following TDM stimulation compared to vehicle treated mice, suggesting that this new treatment strategy has a direct effect on granuloma formation. Moreover, mice treated with anti-IL-1β antibody showed significantly reduced granuloma burden following TDM stimulation compared to mice treated with vehicle or isotype control antibody. Taken together these data suggest that the NLRP3 inflammasome pathway is active in this mouse model of sarcoidosis.

Our findings are limited by the fact that TDM-induced granuloma formation in mice is acute and transient with spontaneous resolution that occurs after 10 days. Furthermore, ultrastructural analysis showed accumulation of macrophages but not epitheloid cells in the center of the evolving granuloma [51]. However, we lack currently any accepted mouse model for sarcoidosis. In our hands the TDM model is superior to all other models that we tested. Similar to granuloma in human sarcoidosis, TDM-induced granuloma are composed of multinucleated giant which express IL-1β and SAA. Moreover, as with sarcoidosis, TDM-induced granuloma is considered to involve mycobacterial PAMPs as a possible trigger in the initial formation of granuloma. Mycobacterial-derived PAMPs have been identified in sarcoid granuloma and Kveim reagent[6, 52] Based on these considerations, we think that the TDM-

induced granuloma model is one of the best currently available models for granuloma formation in sarcoidosis. Future *in vivo* studies are however needed which analyse the effect of NLRP3 inflammasome blockade on already established lung granuloma. Our human studies are limited by the fact that we were not able to detect NLRP3 expression in sarcoid granuloma by immunohistochemistry due to a lack of a specific antibody which gives reliable stainings in formalin fixed tissues. Although our RT-PCT experiments and functional experiments suggest NLRP3 inflammasome activation upregulated in macrophages of patients with severe sarcoidosis and need for immunosuppressive treatment, we cannot exclude that other inflammasome subtypes may additionally be activated. Moreover, since we did not perform PET/CT scanning in our two sarcoid cohorts we cannot provide the information whether NLRP3 inflammasome activation and NLRP3 expression is increased in BAL cells of patients with advanced fibrotic disease and less inflammation.

In conclusion, our studies underscore a role for the NLRP3 inflammasome in sarcoidosis. Our data suggest a pivotal role of NLRP3 inflammasome activation in granuloma formation and demonstrate a beneficial effect of a NLRP3 inflammasome pathway inhibitor on granuloma formation. These data warrant future studies addressing NLRP3 inflammasome inhibition in patients with sarcoidosis. The clinical relevance of inflammasome activation in sarcoidosis pathobiology is currently being explored in an ongoing trial of therapeutic IL-1β blockade in patients with active pulmonary sarcoidosis (www.clinicaltrials.gov; NCT02888080).

REFERENCES

1. Valeyre D, Prasse A, Nunes H, Uzunhan Y, Brillet PY, Muller-Quernheim J. Sarcoidosis. *Lancet* 2014: 383(9923): 1155-1167.
2. Baughman RP, Culver DA, Judson MA. A concise review of pulmonary sarcoidosis. *Am J Respir Crit Care Med* 2011: 183(5): 573-581.
3. Chen ES, Moller DR. Sarcoidosis--scientific progress and clinical challenges. *Nat Rev Rheumatol* 2011: 7(8): 457-467.
4. Spagnolo P, Rossi G, Trisolini R, Sverzellati N, Baughman RP, Wells AU. Pulmonary sarcoidosis. *Lancet Respir Med* 2018: 6(5): 389-402.
5. Moller DR. Potential etiologic agents in sarcoidosis. *Proc Am Thorac Soc* 2007: 4(5): 465-468.
6. Eishi Y. Etiologic link between sarcoidosis and Propionibacterium acnes. *Respir Investig* 2013: 51(2): 56-68.
7. Chen ES, Song Z, Willett MH, Heine S, Yung RC, Liu MC, Groshong SD, Zhang Y, Tuder RM, Moller DR. Serum amyloid A regulates granulomatous inflammation in sarcoidosis through Toll-like receptor-2. *Am J Respir Crit Care Med* 2010: 181(4): 360-373.
8. Vorselaars AD, van Moorsel CH, Deneer VH, Grutters JC. Current therapy in sarcoidosis, the role of existing drugs and future medicine. *Inflamm Allergy Drug Targets* 2013: 12(6): 369-377.
9. Broos CE, Wapenaar M, Looman CWN, In 't Veen J, van den Toorn LM, Overbeek MJ, Grootenboers M, Heller R, Mostard RL, Poell LHC, Hoogsteden HC, Kool M, Wijsenbeek MS, van den Blink B. Daily home spirometry to detect early steroid treatment effects in newly treated pulmonary sarcoidosis. *Eur Respir J* 2018: 51(1).
10. Muller-Quernheim J, Pfeifer S, Mannel D, Strausz J, Ferlinz R. Lung-restricted activation of the alveolar macrophage/monocyte system in pulmonary sarcoidosis. *Am Rev Respir Dis* 1992: 145(1): 187-192.
11. Kline JN, Schwartz DA, Monick MM, Floerchinger CS, Hunninghake GW. Relative release of interleukin-1 beta and interleukin-1 receptor antagonist by alveolar macrophages. A study in asbestos-induced lung disease, sarcoidosis, and idiopathic pulmonary fibrosis. *Chest* 1993: 104(1): 47-53.
12. Steffen M, Petersen J, Oldigs M, Karmeier A, Magnussen H, Thiele HG, Raedler A. Increased secretion of tumor necrosis factor-alpha, interleukin-1-beta, and interleukin-6 by alveolar macrophages from patients with sarcoidosis. *J Allergy Clin Immunol* 1993: 91(4): 939-949.
13. Mikuniya T, Nagai S, Takeuchi M, Mio T, Hoshino Y, Miki H, Shigematsu M, Hamada K, Izumi T. Significance of the interleukin-1 receptor antagonist/interleukin-1 beta ratio as a prognostic factor in patients with pulmonary sarcoidosis. *Respiration* 2000: 67(4): 389-396.
14. Pueringer RJ, Schwartz DA, Dayton CS, Gilbert SR, Hunninghake GW. The relationship between alveolar macrophage TNF, IL-1, and PGE2 release, alveolitis, and disease severity in sarcoidosis. *Chest* 1993: 103(3): 832-838.
15. Prior C, Knight RA, Herold M, Ott G, Spiteri MA. Pulmonary sarcoidosis: patterns of cytokine release in vitro. *Eur Respir J* 1996: 9(1): 47-53.
16. Marshall BG, Wangoo A, Cook HT, Shaw RJ. Increased inflammatory cytokines and new collagen formation in cutaneous tuberculosis and sarcoidosis. *Thorax* 1996: 51(12): 1253-1261.
17. Latz E, Xiao TS, Stutz A. Activation and regulation of the inflammasomes. *Nat Rev Immunol* 2013: 13(6): 397-411.

18. Talreja J, Talwar H, Ahmad N, Rastogi R, Samavati L. Dual Inhibition of Rip2 and IRAK1/4 Regulates IL-1beta and IL-6 in Sarcoidosis Alveolar Macrophages and Peripheral Blood Mononuclear Cells. *J Immunol* 2016: 197(4): 1368-1378.

19. Rastogi R, Du W, Ju D, Pirockinaite G, Liu Y, Nunez G, Samavati L. Dysregulation of p38 and MKP-1 in response to NOD1/TLR4 stimulation in sarcoid bronchoalveolar cells. *Am J Respir Crit Care Med* 2011: 183(4): 500-510.

20. Kern JA, Lamb RJ, Reed JC, Elias JA, Daniele RP. Interleukin-1-beta gene expression in human monocytes and alveolar macrophages from normal subjects and patients with sarcoidosis. *Am Rev Respir Dis* 1988: 137(5): 1180-1184.

21. Bauernfeind F, Hornung V. Of inflammasomes and pathogens--sensing of microbes by the inflammasome. *EMBO Mol Med* 2013: 5(6): 814-826.

22. Hornung V, Bauernfeind F, Halle A, Samstad EO, Kono H, Rock KL, Fitzgerald KA, Latz E. Silica crystals and aluminum salts activate the NALP3 inflammasome through phagosomal destabilization. *Nat Immunol* 2008: 9(8): 847-856.

23. Dostert C, Petrilli V, Van Bruggen R, Steele C, Mossman BT, Tschopp J. Innate immune activation through Nalp3 inflammasome sensing of asbestos and silica. *Science* 2008: 320(5876): 674-677.

24. Cassel SL, Eisenbarth SC, Iyer SS, Sadler JJ, Colegio OR, Tephly LA, Carter AB, Rothman PB, Flavell RA, Sutterwala FS. The Nalp3 inflammasome is essential for the development of silicosis. *Proc Natl Acad Sci U S A* 2008: 105(26): 9035-9040.

25. Ather JL, Ckless K, Martin R, Foley KL, Suratt BT, Boyson JE, Fitzgerald KA, Flavell RA, Eisenbarth SC, Poynter ME. Serum amyloid A activates the NLRP3 inflammasome and promotes Th17 allergic asthma in mice. *J Immunol* 2011: 187(1): 64-73.

26. Niemi K, Teirila L, Lappalainen J, Rajamaki K, Baumann MH, Oorni K, Wolff H, Kovanen PT, Matikainen S, Eklund KK. Serum amyloid A activates the NLRP3 inflammasome via P2X7 receptor and a cathepsin B-sensitive pathway. *J Immunol* 2011: 186(11): 6119-6128.

27. Yu N, Liu S, Yi X, Zhang S, Ding Y. Serum amyloid A induces interleukin-1beta secretion from keratinocytes via the NACHT, LRR and PYD domains-containing protein 3 inflammasome. *Clin Exp Immunol* 2015: 179(2): 344-353.

28. Halle A, Hornung V, Petzold GC, Stewart CR, Monks BG, Reinheckel T, Fitzgerald KA, Latz E, Moore KJ, Golenbock DT. The NALP3 inflammasome is involved in the innate immune response to amyloid-beta. *Nat Immunol* 2008: 9(8): 857-865.

29. Coll RC, Robertson AA, Chae JJ, Higgins SC, Munoz-Planillo R, Inserra MC, Vetter I, Dungan LS, Monks BG, Stutz A, Croker DE, Butler MS, Haneklaus M, Sutton CE, Nunez G, Latz E, Kastner DL, Mills KH, Masters SL, Schroder K, Cooper MA, O'Neill LA. A small-molecule inhibitor of the NLRP3 inflammasome for the treatment of inflammatory diseases. *Nat Med* 2015: 21(3): 248-255.

30. Hunninghake GW, Costabel U, Ando M, Baughman R, Cordier JF, du Bois R, Eklund A, Kitaichi M, Lynch J, Rizzato G, Rose C, Selroos O, Semenzato G, Sharma OP. ATS/ERS/WASOG statement on sarcoidosis. American Thoracic Society/European Respiratory Society/World Association of Sarcoidosis and other Granulomatous Disorders. *Sarcoidosis Vasc Diffuse Lung Dis* 1999: 16(2): 149-173.

31. Prasse A, Katic C, Germann M, Buchwald A, Zissel G, Muller-Quernheim J. Phenotyping sarcoidosis from a pulmonary perspective. *Am J Respir Crit Care Med* 2008: 177(3): 330-336.

32. Prasse A, Zissel G, Lutzen N, Schupp J, Schmiedlin R, Gonzalez-Rey E, Rensing-Ehl A, Bacher G, Cavalli V, Bevec D, Delgado M, Muller-Quernheim J. Inhaled vasoactive intestinal peptide exerts immunoregulatory effects in sarcoidosis. *Am J Respir Crit Care Med* 2010: 182(4): 540-548.

33. Prasse A, Pechkovsky DV, Toews GB, Jungraithmayr W, Kollert F, Goldmann T, Vollmer E, Muller-Quernheim J, Zissel G. A vicious circle of alveolar macrophages and fibroblasts perpetuates pulmonary fibrosis via CCL18. *Am J Respir Crit Care Med* 2006: 173(7): 781-792.

34. Guidry TV, Hunter RL, Jr., Actor JK. Mycobacterial glycolipid trehalose 6,6'-dimycolate-induced hypersensitive granulomas: contribution of CD4+ lymphocytes. *Microbiology* 2007: 153(Pt 10): 3360-3369.

35. Perez RL, Roman J, Roser S, Little C, Olsen M, Indrigo J, Hunter RL, Actor JK. Cytokine message and protein expression during lung granuloma formation and resolution induced by the mycobacterial cord factor trehalose-6,6'-dimycolate. *J Interferon Cytokine Res* 2000: 20(9): 795-804.

36. Bauernfeind F, Rieger A, Schildberg FA, Knolle PA, Schmid-Burgk JL, Hornung V. NLRP3 inflammasome activity is negatively controlled by miR-223. *J Immunol* 2012: 189(8): 4175-4181.

37. Wewers MD, Saltini C, Sellers S, Tocci MJ, Bayne EK, Schmidt JA, Crystal RG. Evaluation of alveolar macrophages in normals and individuals with active pulmonary sarcoidosis for the spontaneous expression of the interleukin-1 beta gene. *Cell Immunol* 1987: 107(2): 479-488.

38. Rolfe MW, Standiford TJ, Kunkel SL, Burdick MD, Gilbert AR, Lynch JP, 3rd, Strieter RM. Interleukin-1 receptor antagonist expression in sarcoidosis. *Am Rev Respir Dis* 1993: 148(5): 1378-1384.

39. Besnard V, Calender A, Bouvry D, Pacheco Y, Chapelon-Abric C, Jeny F, Nunes H, Planes C, Valeyre D. G908R NOD2 variant in a family with sarcoidosis. *Respir Res* 2018: 19(1): 44.

40. Bello GA, Adrianto I, Dumancas GG, Levin AM, Iannuzzi MC, Rybicki BA, Montgomery C. Role of NOD2 Pathway Genes in Sarcoidosis Cases with Clinical Characteristics of Blau Syndrome. *Am J Respir Crit Care Med* 2015: 192(9): 1133-1135.

41. Ziegenhagen MW, Rothe ME, Schlaak M, Muller-Quernheim J. Bronchoalveolar and serological parameters reflecting the severity of sarcoidosis. *Eur Respir J* 2003: 21(3): 407-413.

42. Drent M, Jacobs JA, de Vries J, Lamers RJ, Liem IH, Wouters EF. Does the cellular bronchoalveolar lavage fluid profile reflect the severity of sarcoidosis? *Eur Respir J* 1999: 13(6): 1338-1344.

43. Broos CE, Koth LL, van Nimwegen M, In 't Veen J, Paulissen SMJ, van Hamburg JP, Annema JT, Heller-Baan R, Kleinjan A, Hoogsteden HC, Wijsenbeek MS, Hendriks RW, van den Blink B, Kool M. Increased T-helper 17.1 cells in sarcoidosis mediastinal lymph nodes. *Eur Respir J* 2018: 51(3).

44. Zielinski CE, Mele F, Aschenbrenner D, Jarrossay D, Ronchi F, Gattorno M, Monticelli S, Lanzavecchia A, Sallusto F. Pathogen-induced human TH17 cells produce IFN-gamma or IL-10 and are regulated by IL-1beta. *Nature* 2012: 484(7395): 514-518.

45. Deng J, Yu XQ, Wang PH. Inflammasome activation and Th17 responses. *Mol Immunol* 2019: 107: 142-164.

46. Huho A, Foulke L, Jennings T, Koutroumpakis E, Dalvi S, Chaudhry H, Chopra A, Modi A, Rane N, Prezant DJ, Sheehan C, Yucel R, Patel M, Judson MA. The role of serum amyloid A staining of granulomatous tissues for the diagnosis of sarcoidosis. *Respir Med* 2017: 126: 1-8.

47. Bargagli E, Magi B, Olivieri C, Bianchi N, Landi C, Rottoli P. Analysis of serum amyloid A in sarcoidosis patients. *Respir Med* 2011: 105(5): 775-780.

48. Rothkrantz-Kos S, van Dieijen-Visser MP, Mulder PG, Drent M. Potential usefulness of inflammatory markers to monitor respiratory functional impairment in sarcoidosis. *Clin Chem* 2003: 49(9): 1510-1517.

49. Haneklaus M, Gerlic M, Kurowska-Stolarska M, Rainey AA, Pich D, McInnes IB, Hammerschmidt W, O'Neill LA, Masters SL. Cutting edge: miR-223 and EBV miR-BART15 regulate the NLRP3 inflammasome and IL-1beta production. *J Immunol* 2012: 189(8): 3795-3799.

50. Neudecker V, Haneklaus M, Jensen O, Khailova L, Masterson JC, Tye H, Biette K, Jedlicka P, Brodsky KS, Gerich ME, Mack M, Robertson AAB, Cooper MA, Furuta GT, Dinarello CA, O'Neill LA, Eltzschig HK, Masters SL, McNamee EN. Myeloid-derived miR-223 regulates intestinal inflammation via repression of the NLRP3 inflammasome. *J Exp Med* 2017: 214(6): 1737-1752.

51. Soler P, Bernaudin JF, Basset F. Ultrastructure of pulmonary granulomatosis induced in rats by intravenous complete Freund's adjuvant. *Virchows Arch A Pathol Anat Histol* 1975: 368(1): 35-50.

52. Schupp JC, Tchaptchet S, Lutzen N, Engelhard P, Muller-Quernheim J, Freudenberg MA, Prasse A. Immune response to Propionibacterium acnes in patients with sarcoidosis--in vivo and in vitro. *BMC Pulm Med* 2015: 15: 75.

Table 1 Clinical characteristics of sarcoidosis patients and control subjects

	HV	SSc	SARC	Sarcoidosis lung disease activity		
				mild	moderate	severe
Total subjects	19	6	19	5	3	11
Female	13	5	7	3	0	4
Male	6	1	12	2	3	7
Age (yrs)	29 ± 10	49± 14	48 ± 14*	47 ± 19	39 ± 7	51 ± 13
Chest x-ray type I/II/III/IV	N/A	N/A	2/ 14/ 1/ 2	2/ 3/ 0/ 0	0/ 3/ 0/ 0	0/ 8/ 1/ 2
FVC (%)	115 ± 5	71± 22	93 ± 23*	118 ± 9	93 ± 20	82 ± 18#
DLCO (%)	N/A	43± 21	74 ± 20	85 ± 23	86 ± 21	65 ± 13
Need for IS treatment N/Y	N/A	6Y	5N /12Y	4 N /1Y [1)]	3 N	11 Y
BAL differential						
Macrophages (%)	87 ± 6	80±13	55 ± 20*	64 ± 27	61 ± 23	49 ± 16
Lymphocytes (%)	10 ± 6	8±8	43 ± 20*	34 ± 27	38 ± 23	48 ± 16
Neutrophils (%)	2 ± 1	10±7	2 ± 1	2 ± 2	1 ± 0	2 ± 1
BAL cell recovery cellx10^6/100 ml	6.2 ± 2.4	17.0 ± 5.0	14.4 ± 8.1*	7.1 ± 4.8	15.5 ± 8.2	17.4 ± 7.7#
Neopterin (nmol/l)	N/A	N/A	15.7 ± 8.5	12.2 ± 6.5	9.4 ± 2.5	18.9 ± 9.1
sIL-2R (U/ml)	N/A	N/A	1646 ± 1702	963 ± 805	744 ± 219	2203 ± 2032

Definition of abbreviations: HV: healthy volunteer;SSc: scleroderma patients, SARC: patients with sarcoidosis. BAL: bronchoalveolar lavage; N/A: not applicable. FVC: forced vital capacitiy; DLCO: diffusing capacity of the lungs for carbon monoxide. IS = Immunosuppressive treatment. N= no treatment. Y= treatment. Values shown as mean ± standard deviation. Statistical comparisons between groups were done using the Mann-Whitney U test. * $p< 0.05$ in the comparison healthy volunteers versus sarcoid patients. # $p<0.05$ in the comparison sarcoid patients with mild disease versus severe disease. [1)]due to eye involvement, not due to pulmonary activity.

Figure 1

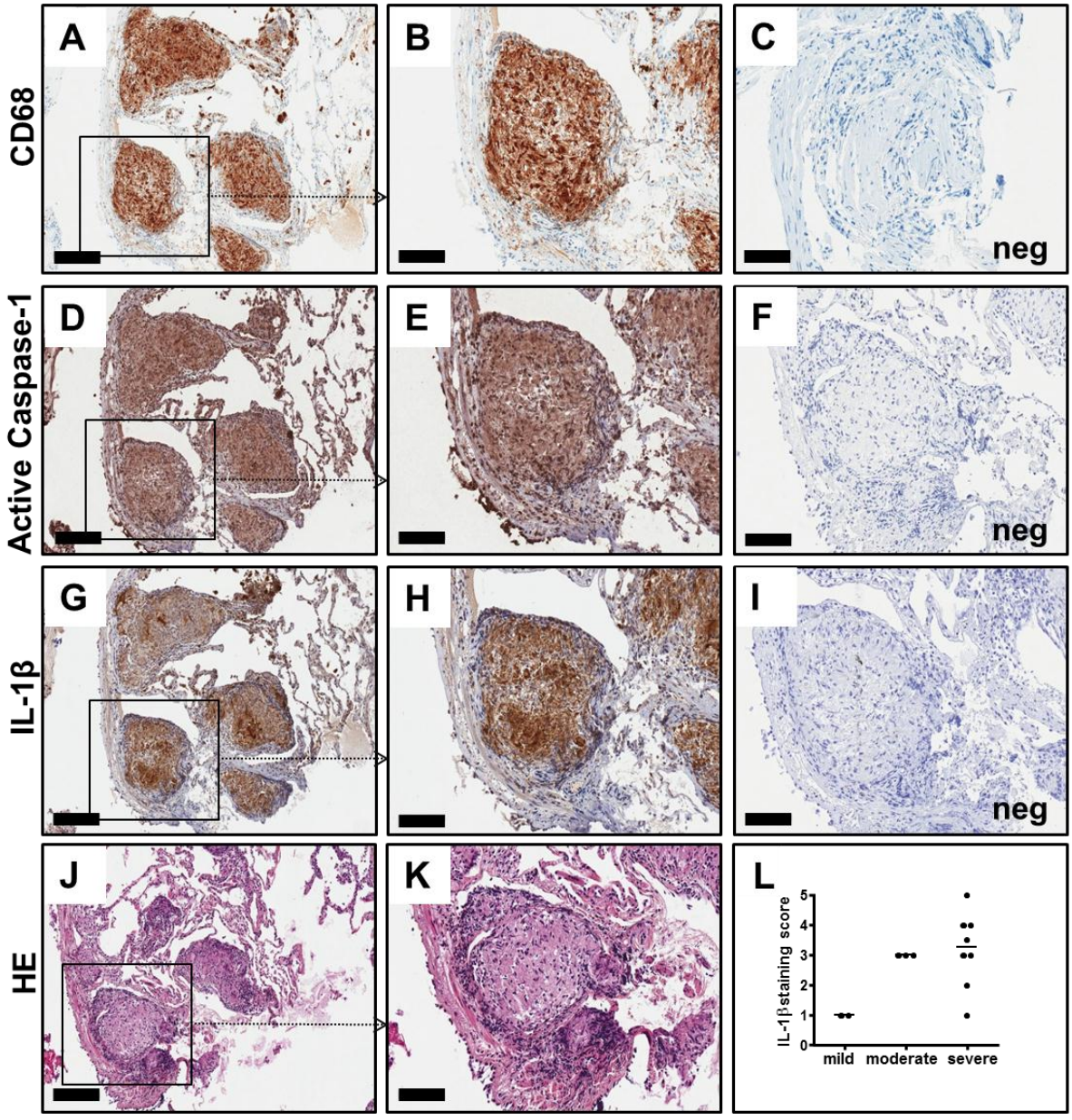

Figure 1. Evidence for inflammasome and IL-1β pathway activation in sarcoid lung granulomas. (A-K) Representative photomicrographs of consecutive sections of tissues derived by transbronchial biopsy (TBB) from a sarcoid patient with severe lung disease activity. (A-I) TBB tissue was immunohistochemically stained using antibodies against the macrophage lineage marker CD68 (A,B), activated caspase-1 (D,E) and IL-1β (G,H). (C, F, I) Negative control stainings were obtained by applying respective isotype control antibodies. (J, K) TBB tissue was stained with hematoxylin eosin (H&E) for histopathological assessment, indicating non-necrotizing sarcoid granuloma. Bar in left panels 100 μm and in middle and right panels 200 μm. (L) Quantification of IL-1β immunoreactivity in lung granuloma is depicted in relation to pulmonary disease activity. IL-1β staining was blindly scored semi-quantitatively for TBBs derived from 13 patients.

Figure 2

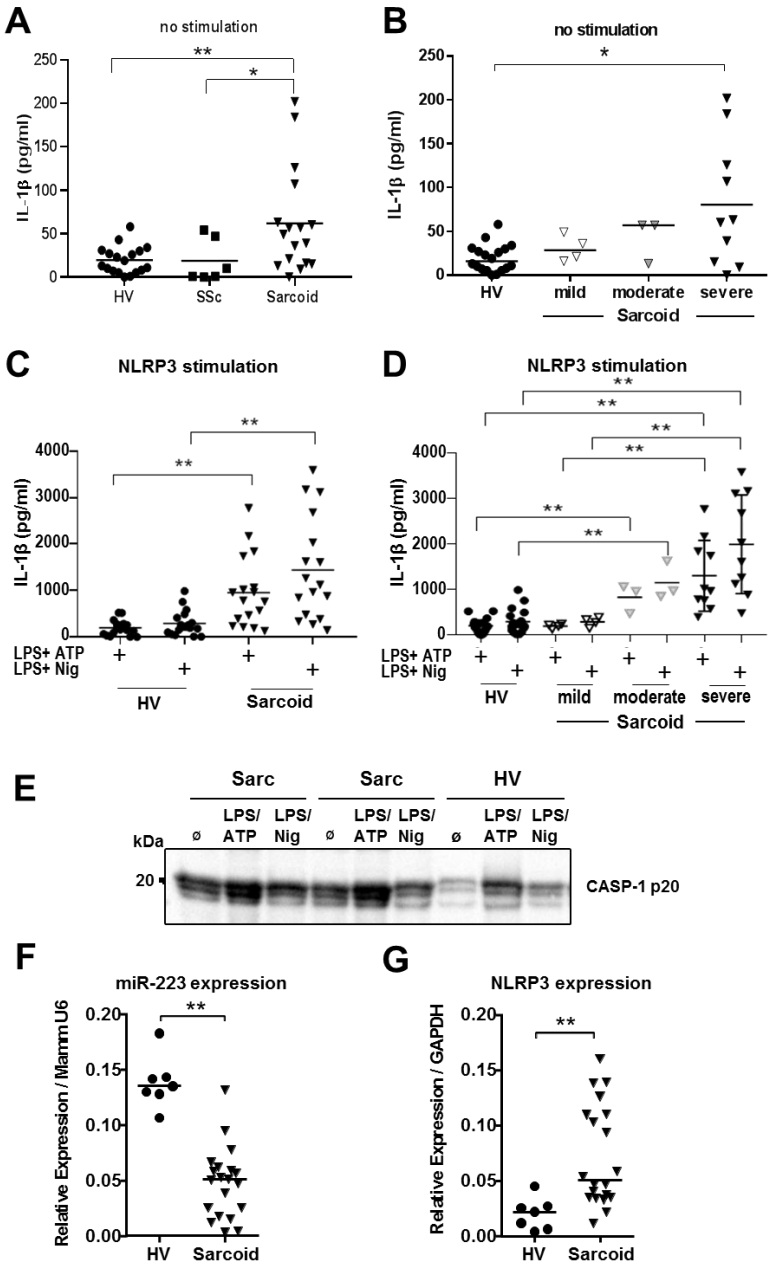

Figure 2. Evidence for an activated NLRP3 inflammasome pathway in BAL cells from sarcoid patients. *(A-E) BAL cells from HV, patients with scleroderma ILD (SSc) or patients with sarcoidosis (Sarcoid) were left unstimulated for 6h (A,B) or stimulated for 6h with LPS + nigericin or LPS + ATP to activate the NLRP3 inflammasome (C-E) and levels of IL-1β and the cleaved subunit caspase-1 p20 were measured in the cell culture supernatants by ELISA and Western blot. Panels A, C depict IL-1β levels from HV (n=18), sarcoid patients (n=17), and patients with SSc-ILD (n=6) and panels B,D depict IL-1β levels from sarcoid patients across pulmonary disease activity. E) Representative immunoblot analysis for the cleaved caspase-1 subunit p20, which results from caspase-1 activation by the inflammasome. (F, G) In an additional study, alveolar macrophages were sorted from BAL cells from 20 severe sarcoid patients with progressive disease and need for combined immunosuppressive treatment and 7 HV and relative miR-223 expression to MammU6 (F) and NLRP3 relative to GAPDH expression (G) was determined by RT-PCR. The bar depicts the median. *p<0.05, **p<0.01, Mann-Whitney U test.*

]

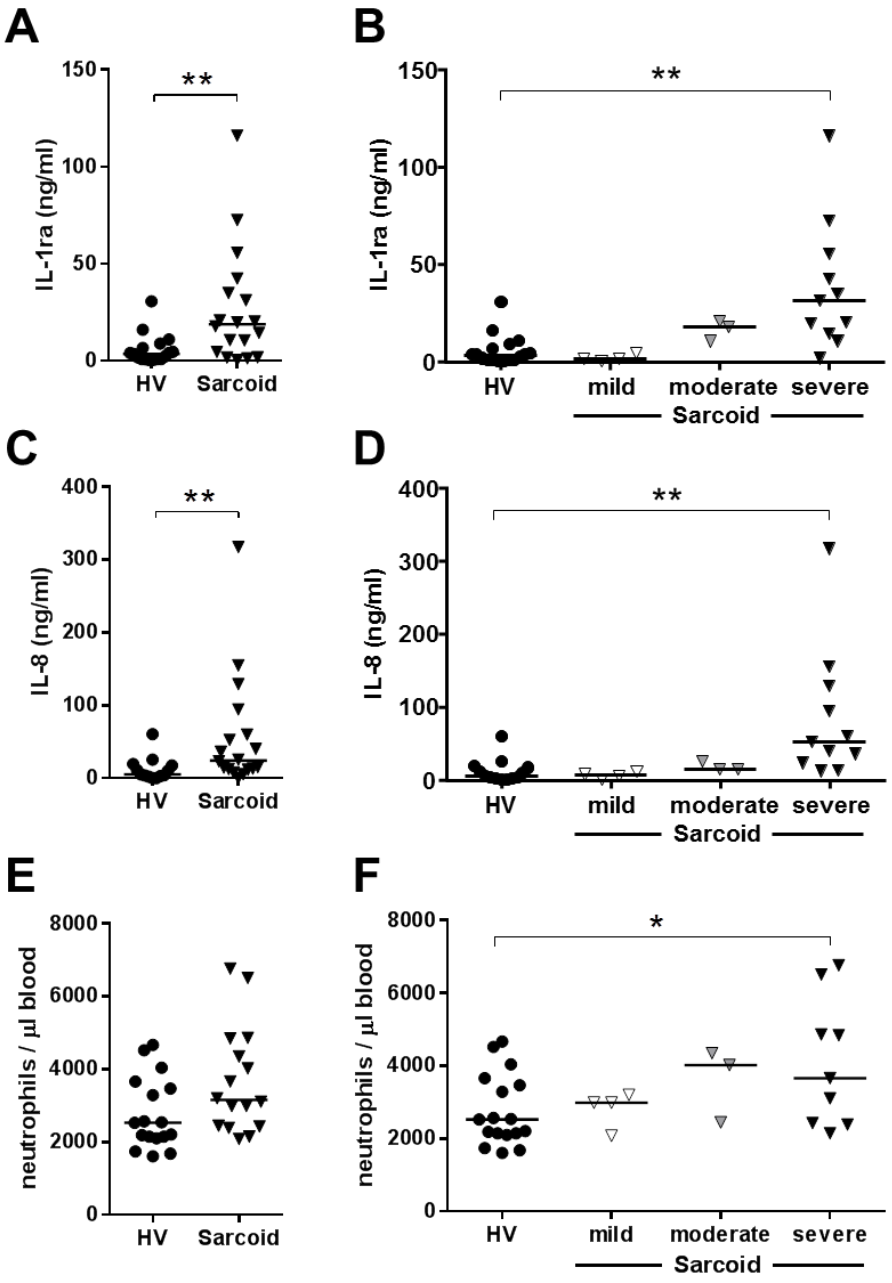

Figure 3. Constitutive IL-1ra and IL-8 release from BAL cells and increased neutrophil counts in sarcoidosis are indicative of IL-1β pathway activation. *(A-D) BAL cells from HV or sarcoid patients were cultured without further stimulation for 24h and levels of IL-1ra (A, B), IL-8 (C, D) were measured in the conditioned medium. Panel A depicts IL-1ra production of BAL cells from HV (n=17) and sarcoid patients (n=18) and panel B depicts IL-1ra production of BAL cells from sarcoid patients across pulmonary disease activity. Panel C and D depict IL-8 production from BAL cells accordingly (HV, n=13; SARC, n=18). (E, F) Blood neutrophil counts determined by FACS for HV (n=17) and sarcoid patients (n=16) and in accordance to pulmonary disease activity. The bar depicts the median. *p<0.05, **p<0.01, Mann-Whitney U test.*

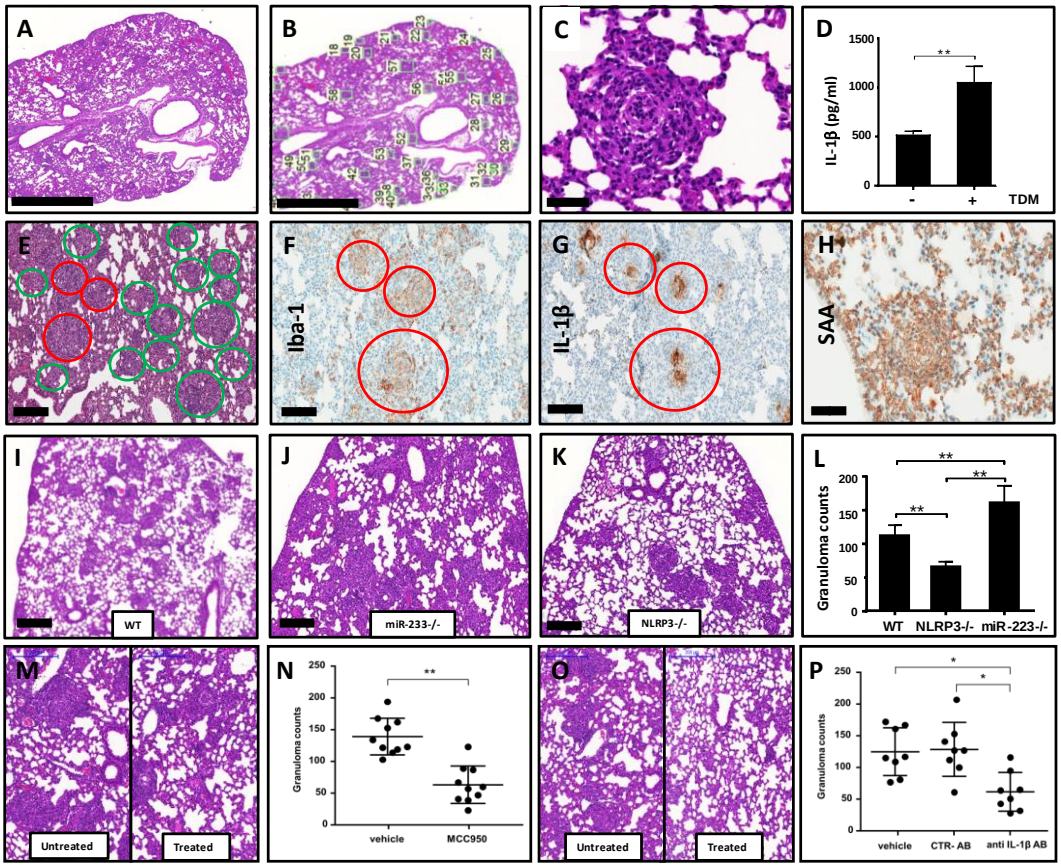

Figure 4. TDM induced pulmonary granuloma in mice resemble human sarcoid granuloma: Involvment of the NLRP3 inflammasome pathway and reduced pulmonary granuloma burden in mice treated with compounds targeting the NLRP3 inflammasome. *(A) H&E stain of lung harvested on day 7 from C57/BL6 wildtype (WT) mice challenged with TDM. (B) Counting strategy for granuloma burden of the left lobe of the lung. (C) High magnification of typical TDM-induced granulomas in mouse lung. (D) IL-1β release from BAL cells stimulated ex vivo with LPS/nigericin (6 h) was determined in the supernatants. (E) H&E stained section of lung granulomas, red circles indicate the sites of higher magnification in F and G. what about green circles (F-H) Immunohistochemistry of the TDM induced granuloma using antibodies against the mouse macrophage lineage marker Iba-1 (F), IL-1β (G) or SAA what do red circles denote (H). (I-K) H&E stains of lung tissues from WT mice (I), miR-223-/- mice (J) and NLRP3-/- mice (K) 7d after TDM injection (each 6 replicates). (L) Granuloma counts of lung tissues from WT, miR-223 -/- mice and NLRP3-/- mice. Individual values and mean ± SD are shown. **p<0.01, unpaired t-test. (M) H&E stains of lungs from TDM-treated C57/BL6 wildtype mice treated with vehicle or the NLRP3 inflammasome pathway inhibitor MCC950 (each 2 replicates). (N) Reduced granuloma counts in lung tissues from MCC950-treated compared to vehicle-treated mice. Individual values and mean ± SD are shown. *p<0.05, unpaired ANOVA. (O) H&E stains of lung from TDM-treated C57/BL6 wildtype mice treated with isotype control antibody or anti-IL-1β antibody. (P) Significantly reduced granuloma counts in lung tissues from anti-IL-1β-treated compared to mice treated with isotype control antibody or vehicle (each 8 replicates). Individual values and mean ± standard deviation are shown. *p<0.05, unpaired ANOVA. Bar in panels A,B, 1000 μm; Bar in panel C 10 μm; bar in panel. E-G, and I-K 500 μm.*

Supplement to

The NLRP3 inflammasome pathway is activated in sarcoidosis and involved in granuloma formation

Christine Huppertz[1†], Benedikt Jäger[2,3,4†], Grazyna Wieczorek[1], Peggy Engelhard[3, 4], Stephen J. Oliver[1], Franz-Georg Bauernfeind[5], Amanda Littlewood-Evans[1], Tobias Welte[7,8], Veit Hornung[6], Antje Prasse[2,4,7,8,*]

Supplementary Methods

Bronchoalveolar lavage, transbronchial biopsies and laboratory chemistry

Bronchoalveolar lavage (BAL) was performed in healthy volunteers and sarcoidosis patients as part of their routine diagnostic work-up in accordance to a standardized protocol.[1-3] The BAL was pooled, filtered through two layers of gauze, and centrifuged at 500 g for 10 minutes at 4°C. The cells were counted and cell smears were stained with May-Grunwald-Giemsa stain (Merck, Germany) for the cell differentials. Following this, BAL cells were further processed for functional assays, sorting of alveolar macrophages and RNA extraction as described below. In addition, transbronchial biopsies (TBB) were obtained from sarcoid patients during the routine diagnostic work-up and further processed for histopathology and immunohistochemistry. Skin biopsies from sarcoid patients were also obtained within the routine diagnostic work-up at the Department of Dermatology, University Medical Center Freiburg. The standard laboratory chemistry parameters, serum sIL-2R and serum neopterin, were measured by routine laboratory chemistry at the University Medical Center Freiburg using a standardized protocol.[1] Serum levels of SAA were determined by ELISA (Invitrogen/Thermo Fisher Scientific, USA).

Histopathology and immunohistochemistry of human biopsies

Tissues from human transbronchial biopsies or skin biopsies were fixed for 24 hours in 10% normal buffered formalin, dehydrated through graded alcohol and xylene and embedded in paraffin. Three-µm-thick sections were cut and stained with hematoxylin and eosin (H&E) and immunohistochemically, using primary antibodies specific for human macrophage lineage marker CD68 (clone KP-1, Dako, Denmark, 1:500), for cleaved caspase-1, D210 (rabbit polyclonal, YC0002, ImmunoWay Biotechnology, USA, 1:50) and IL-1β (goat polyclonal, raised against *E. coli*-derived recombinant human IL-1β /IL-1F2 Ala117-Ser269, AF-201-NA, R&D Systems, UK, 1:10) and secondary reagents, including for CD68, a goat-anti mouse-biotinylated antibody (Vector Laboratories, USA, 1:200); for caspase-1, the Envision+ system anti-rabbit (Dako, Ready to use kit); and for IL-1β, a horse anti-goat-biotinylated antibody (Vector Laboratories, 1:200). Details of the methods are provided in table below. Negative control staining was performed using matched concentrations of isotype control antibodies. Sections from human healthy skin and tonsils were stained in parallel. To further assess specificity of the cleaved/active caspase-1 antibody, staining was performed on paraffin-embedded THP-1 cells with and without prior stimulation with 100

ng/ml LPS for 4h. Human skin biopsies and TBB samples were examined blindly and semiquantitatively scored for IL-1β staining intensity: 0 – no cells, 1 - very few cells, 2 - few cells, 3 - moderate number of cells, 4 - many cells, 5 - extensive number of cells.

All biopsy samples were digitalized using ScanScope XT slide scanner (Aperio, Leica Biosystems, Switzerland).

Primary antibodies and methods used for IHC

Marker	Clone	Vendor	Procedure	Pretreatment	Dilution/ Conc.	Incubation	Detection
CD68	KP-1	Dako	Ventana	sCC1	1:500	1 hour, 37°C	DAB Map
Caspase-1,cleaved	Rabbit pAb	Immuno-way YC0002	Manual	borate buffer MW 45 min	1:50 20ug/ml	ON, +4°C	Envision HRP
IL-1 beta	Goat pAb	R&D Systems AF-201-NA	Manual	Envision Flex low, PT-Module 20 min	1:10 10ug/ml	1 hour, RT	ABC-HRP

NLRP3 inflammasome activation of BAL cells

IL-1β production by BAL cells was assessed following NLRP3 inflammasome stimulation. Human BAL cells were cultured in macrophage SFM/Gibco medium (serum free medium; Life technologies) supplemented with 1% penicillin/streptomycin (Biochrom). Human BAL cells (10^5 cells/100µl media; 96-well plates) were stimulated with 1µg/ml LPS (Fluka Biochemika) for 4h followed by 10µM nigericin (Sigma Aldrich) or 1mM ATP (Sigma Aldrich) for a further 2h. Cell supernatants were collected 6h after stimulation to determine levels of IL-1β release by ELISA and Western Blot. The concentration of IL-1β was determined using an ELISA (Human IL-1β/ IL-1F2 DuoSet, R&D) according to the manufacturer's instructions.

Determination of cytokine production by BAL cells following SAA stimulation.

Human BAL cells were cultured at 10^6 cells/ml in 24-well plates in 1 ml RPMI 1640 medium supplemented with 2% human serum and 1% penicillin/streptomycin and stimulated with or without 1µg/ml SAA (recombinant human apo-SAA, PeproTech, Germany). Peripheral blood mononuclear cells (PBMCs) were obtained by Ficoll gradient and cultured under the same conditions. Conditioned medium was harvested after 24h and stored at -80°C. The concentrations of IL-1β , IL-1ra, IL-8 and TNF-α in the conditioned medium were determined by ELISA (all R&D Duosets) or by homogenous time resolved fluorescence (HTRF; Cisbio Bioassays, France) as specified in the manufacturers' instructions.

Immunoblot analysis of caspase-1p20 activity and active IL-1β release

BAL cells were stimulated with the NLRP3 activation protocol described above and supernatants were precipitated with methanol/chloroform. Upon centrifugation, the upper phase was removed and methanol added to the lower phase prior to another centrifugation step. The supernatant was discarded and the pellet was incubated at 55 °C for 10 minutes and resuspended in Laemmli-buffer. Samples were separated using 15% SDS-PAGE gels and transferred to polyvinylidene difluoride membranes. Cleaved caspase-1 (p20) was detected using primary antibody rabbit mAb cleaved caspase-1 (Asp297) (D57A2) (1:200) (Cell Signalling Technology) and IL-1β was detected using primary rabbit polyclonal anti IL-1β antibody (1:1000) (Abcam, ab2105) with the secondary antibody goat anti-rabbit (H+L)-HRP conjugate (1:3000) (BioRad Laboratories). Enhanced chemiluminescence (ClarityTM Western ECL Substrate/BioRad) was used for detection with ChemiDocTM MD Imaging System (BioRad).

MicroRNA analysis and RT-PCR

Alveolar macrophages were sorted from BAL cells from an additional cohort of sarcoid patients and healthy volunteers on a MoFlo Astrios/Beckman Coulter cell sorter based on cell characteristics in the forward/sideward scatter and typical autofluorescence of AMs. In all experiments purity of sorted macrophages exceeded 99%. Total cellular miRNA from 106 sorted AMs was isolated using mirVana™ isolation kit (Thermo Fisher Scientific) and tailed using poly(A) polymerase (Fermentas). Poly(A) RNA was treated with DNAse I (Fermentas) and reverse transcribed with M-MuLV reverse transcriptase (Fermentas) using a PolyT adapter (5′-GCGAGCACAGAATTAATACGACTCACTATAGG(T)18VN-3′). The obtained cDNA was analyzed by Real-Time PCR (Light Cycler/Roche) with the following primers: huNLRP3 (5′-AGAATGCCTTGGGAGACTCA-3′ and 5′-CAGAATTCACCAACCCCAGT-3′), resulting in a 93 bp product, exon 6/7 overlapping; miR-223 (5′-TGTCAGTTTGTCAAATACCCCA-3′ and 5′-GCGAGCACAGAATTAATACGAC-3′), resulting in a 72 bp product (consisting of mir-223 mature sequence and the PolyT adapter); GAPDH (5`-ACAGTCAGCCGCATCTTCTT-3` and 5`-GTTAAAAGCAGCCCTGGTGA-3`) and MammU6 (hsaU6F 5´-AAATTCGTGAAGCGTTCCAT-3´and uni-R 5`-GCGAGCACAGAATTAATACGAC-3`) as reference. The expression of NLRP3 and of

miR-223 was normalized to GAPDH expression or MammU6 expression, respectively, and plotted as arbitrary units on a linear scale.[4]

Isolation of monocytes from peripheral blood mononuclear cells (PBMC)

Human PBMCs were isolated from human blood of healthy volunteers and patients with sarcoidosis by density gradient centrifugation in Ficoll-Paque™ PLUS / GE Healthcare-Life Sciences medium. Human monocytes were isolated from PBMCs of healthy volunteers and patients with sarcoidosis using a commercially available EasySep™ Human Monocyte enrichment kit (StemCell Technologies).

Testing NLRP3 inflammasome activation in monocytes

Monocytes from 19 sarcoid patients and 18 healthy volunteers (same cohort as BAL cells) were isolated as described above and immediately plated at a concentration of $1x10^6$/well in RPMI 1640 medium supplemented with 10% FCS and 1% penicillin/streptomycin and stimulated for 4 hours with either LPS (Fluka Biochemika) (1µg/ml), SAA (recombinant human apo-SAA, PeproTech, Germany) (1µg/ml). After 4h of culture supernatants were harvested and stored at -80°C for IL-1β cytokine measurement by ELISA (R&D Duoset).

Testing the effect of NLRP3 inflammasome inhibition in SAA stimulated monocytes

Human CD14 monocytes from healthy volunteer-derived PBMCs were isolated as described above and stimulated at 10^5 cells/ 200 µl in 96 well plates with or without 1 µg/ml SAA (recombinant human apo-SAA, PeproTech, Germany) for 24 h. Pralnacasan (VX-740) (0.01µM, 0.1µM, 1µM and 10µM), MCC950 (Tocris) (0.01µM, 0.1µM, 1µM and 10µM) or dimethylsulfoxide control were added 30 min prior to SAA.[5] IL-1β production following SAA stimulation was measured in the conditioned medium by homogenous time resolved fluorescence (HTRF; Cisbio Bioassays, France) as specified in the manufacturers' instructions.

Animal studies

NLRP3 -/- mice (B6 strain background) were kindly provided by Dr. Dixit from Genentech.[6] MiR-223 -/- mice (B6.Cg-Ptprca Mir223tm1Fcam/J) (JAX stock #013198)[7] their

respective wildtype (B6.SJL-Ptprca Pepcb/BoyJ) (JAX stock #002014)[8-10] control mice and wildtype (WT) control mice (C57BL/6J) (JAX stock #000664) were purchased from the Jackson Laboratory/USA. All mouse procedures were carried out in accordance to Home Office German regulations and the Animals (Scientific Procedures) Act 1986 and were approved by the respective local Ethical Review Body (Regierungspräsidium Freiburg, Germany (AZ: 35/9185.81/G-07/05; AZ: 35-9185.81/G-10/38) and LAVES, Oldenburg, Germany (AZ: 33.19-42502-04-15/1861; AZ: 33.19-42502-04-15/2018).

Murine pulmonary granuloma model induced by trehalose 6,6'-dimycolate (TDM)

TDM (Enzo Life Sciences GmbH, Germany) from mycobacterium tuberculosis was prepared in a water in oil emulsion using incomplete Freund`s Adjuvant (IFA: vehicle fluid: phosphate buffered saline with 3.2% incomplete Freund`s-Adjuvant (Sigma Aldrich) and 0.2% Tween80 (Sigma Aldrich) as described.[11,12] Six to twelve weeks old NLRP3-/-, miR-223-/-, B6.SJL-Ptprca Pepcb/BoyJ (WT) and C57BL/6J (WT) mice were intravenously injected via the tail vein with 1 µg TDM in 10 µl water in oil emulsion (IFA/PBS and 0.2% Tween80)/ g body weight with the only exception of miR-223-/- mice which received 0.5 µg TDM in 10 µl water in oil emulsion (IFA/PBS and 0.2% Tween80)/g body weight. To assess pulmonary granuloma formation, lungs were harvested on day 7 after TDM injection for all studies (n=6 per group). For IL-1β production by BAL cells after NLRP3 inflammasome activation, mice were sacrificed on day 3 and BAL was performed as described.[13] Six to twelve weeks old C57BL/6J WT mice (n=10 per group) were administered vehicle (PBS) or MCC950, a NLRP3 inflammasome pathway inhibitor, at 10 mg/kg intraperitoneally on day 0, 1, 2, 4, and 6 after TDM injection. In an additional experiment, six to twelve weeks old C57BL/6J WT mice (n=8 per group) were administered subcutaneously with either vehicle (PBS), isotype control antibody anti-cyclosporine (Novartis) [200µg/mouse] or anti-IL1β antibody (Novartis) [200µg/mouse] on day -1 and again 3 days after TDM injection.

Histopathology and immunohistochemistry of mouse lung tissue

Murine lungs were fixed in 10% normal buffered formalin for 24 hours, cut to tissue sections, dehydrated overnight and embedded in paraffin. Paraffin tissue sections from murine lung lobes (3µm) were stained with H&E and immunohistochemically using antibodies specific for mouse macrophage lineage marker Iba-1 (Wako Chemicals USA Inc., USA, 1:500), mouse IL-1β (Abcam, UK, 1:800), and SAA (Novus Biologicals, UK, 1:150).

Granuloma load per lung section was counted semi-quantitatively as exemplified in the results section. All biopsy samples were digitalized using ScanScope XT slide scanner (Aperio, Leica Biosystems, Switzerland) or Mirax Scan 150 BF/FL (Zeiss, Germany).

Primary antibodies and methods used for IHC

Marker	Clone	Vendor	Procedure	Pretreatment	Dilution/ Conc.	Incubation	Detection
Iba-1	Rabbit pAB	Wako	Ventana	sCC1	1:500	1 hour, 37^{o}C	DAB Map
IL-1b	Rabbit pAb	Abcam	Ventana	sCC1	1:800	3 hours, 37^{o}C	OmniMap +TSA HQ
SAA	Reu86.1	Novus	Ventana	sCC1	1:150	1 hour, RT	OmniMap

Statistics

Statistical analyses were performed with Graph Pad Prism Software v6.01. Comparisons between groups from clinical data was done by Mann-Whitney U test, assuming non-parametric, non-Gaussian distribution, and by unpaired t-test or ANOVA for preclinical data as specified in the figure legends. To assess relationships and potential correlation between 2 parameters, r2 values were determined using the linear regression function in Graph Pad Prism Software. For clarity, in the figures, 2 stars denote anything with a significance of $p< 0.01$, while the precise p values are mentioned in the results section (unless they reach levels of $p<0.0001$.)

Supplementary Results

Upregulated SAA levels in sarcoid patients perpetuate NLRP3 inflammasome activity

As SAA has been proposed as a main driver in the pathogenesis of sarcoidosis and also as an activator of the NLRP3 inflammasome, we analyzed the expression and effects of SAA in the context of the NLRP3 inflammasome pathway. We found that serum levels of SAA were significantly increased in sarcoid patients in comparison to HV ($p= 0.0497$, Fig. S6A). Upon ex vivo stimulation with SAA, sarcoid BAL cells, especially those derived from the patients with severe lung disease, elicited significantly higher IL-1β levels than HV BAL cells ($p= 0.0184$, Fig. S6B and data not shown). Furthermore, SAA-induced IL-1β release from PBMCs derived from sarcoid patients versus HV was also significantly higher ($p= 0.0182$, Fig. S6C). In order to confirm SAA as an activator of the NLRP3 inflammasome as was recently postulated, we tested the effects of the published NLRP3 inflammasome pathway inhibitor MCC950 and an inhibitor of caspase-1, VX-740 on SAA-mediated IL-1β release of CD14+ monocytes isolated from peripheral blood from healthy donors. Both inhibitors were able to reduce IL-1β release from the SAA-stimulated monocytes in a dose-dependent manner (Fig. S6D).

Supplementary Figure S1

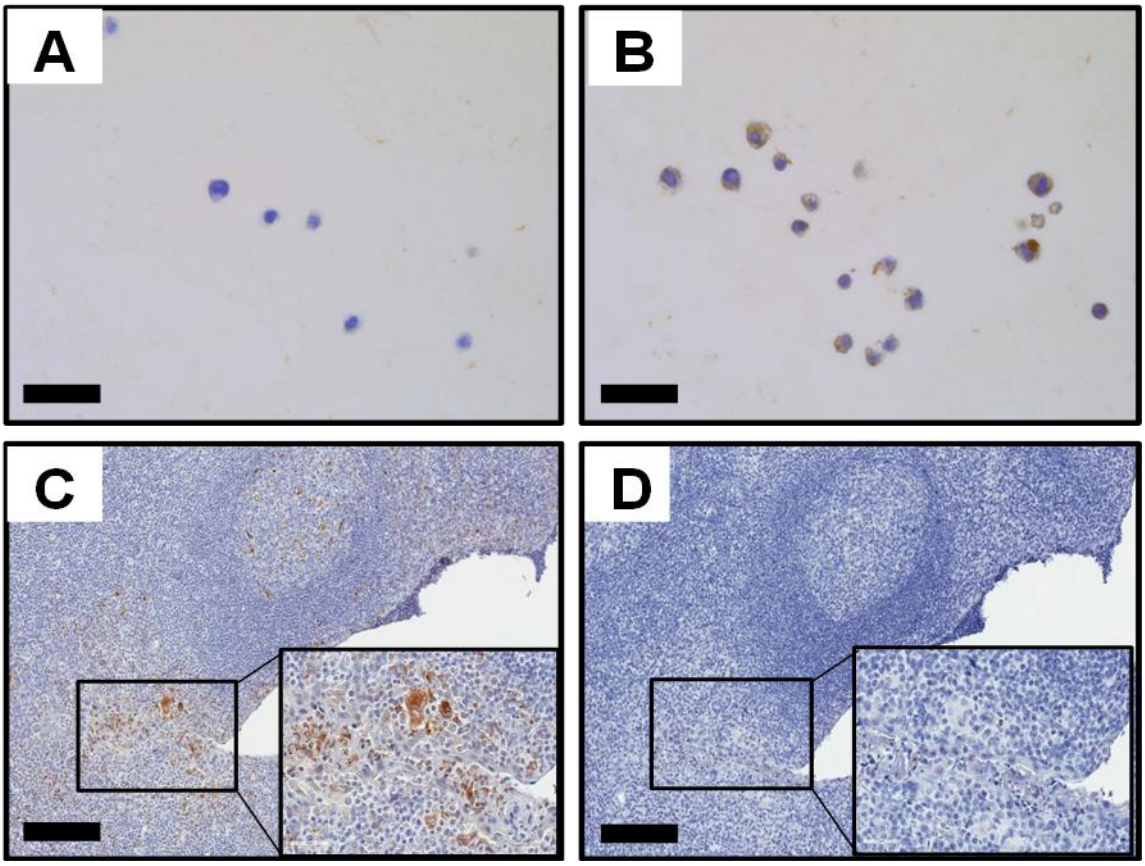

Figure S1: Additional characterization of active caspase-1 antibody*. (A,B) THP-1 cells were left unstimulated (A) or stimulated with LPS (100ng/ml) for 4 h (B), paraffin-embedded, and stained immunohistochemically using an antibody against activated caspase-1. The antibody staining is only positive for LPS stimulated THP-1 cells which express active (cleaved) caspase-1 in the cytoplasm. The scale bar represents 50 µm. (C,D) Representative photomicrographs of consecutive sections of human tonsils stained immunohistochemically using an antibody against CD68 (C) or activate caspase-1 (D). Macrophages from human tonsil tissue are negative for active caspase-1. The scale bar represents 200 µm.*

Supplementary Figure S2

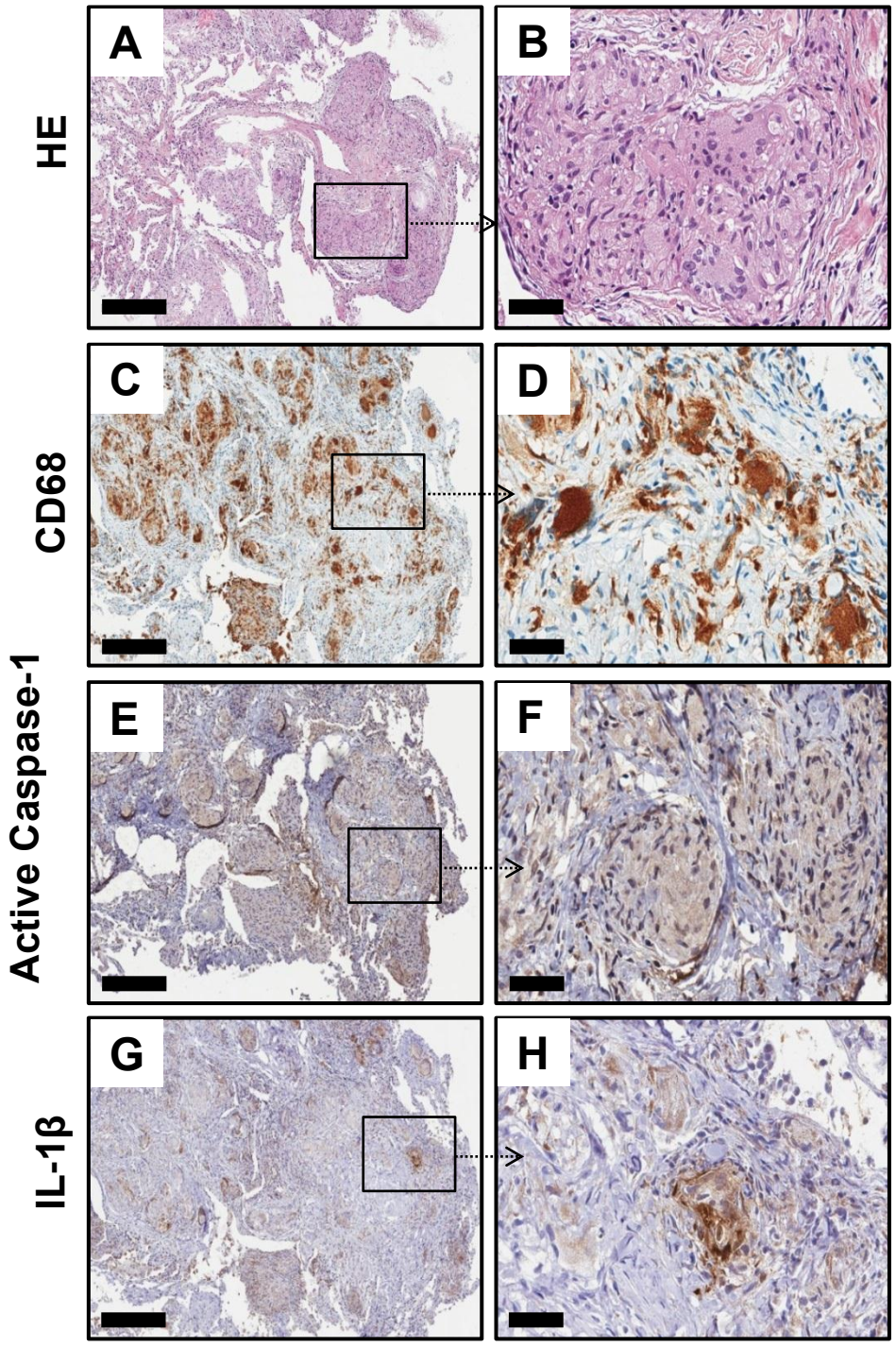

Figure S2: Evidence for inflammasome and IL-1β pathway activation in sarcoid lung granulomas. *(A-H) Representative original photomicrographs of consecutive sections of tissues derived by transbronchial biopsy (TBB) from an additional sarcoid patient (severe disease and different from the patient in Fig. 1). (A, B) TBB tissue was stained with hematoxylin eosin (H&E) for histopathological assessment. (C-H) TBB tissue was stained immunohistochemically using antibodies against the macrophage lineage marker CD68 (C,D), activated caspase-1 (E,F), or IL-1β (G,H). The scale bar represents 300 μm (panel A,C,E,G) and 50 μm (panel B,D,F,H).*

Supplementary Figure S3

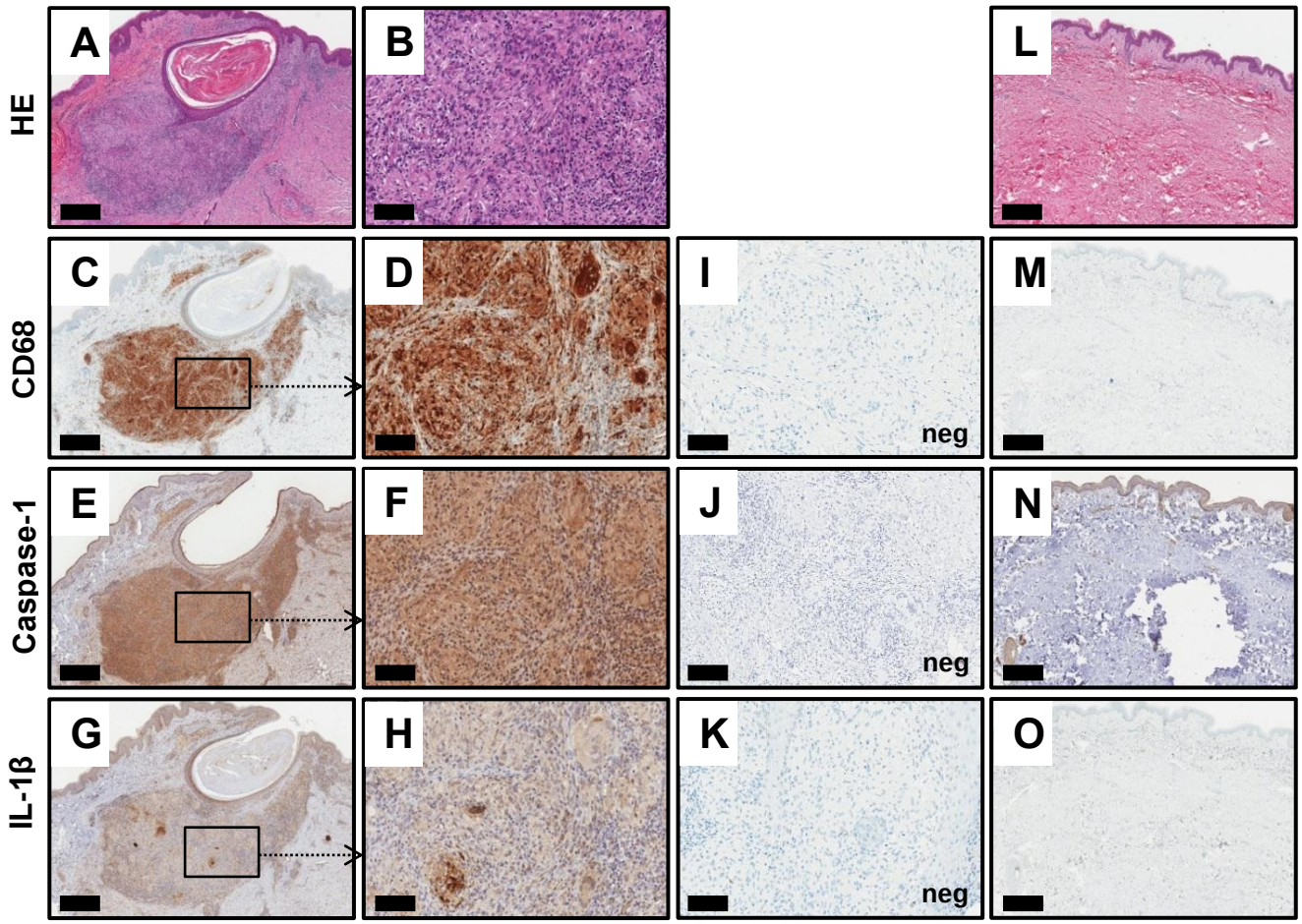

Figure S3: Evidence for inflammasome and IL-1β pathway activation in sarcoid skin granulomas. *(A-K) Representative original photomicrographs of skin biopsy tissue from a sarcoid patient. (A,B) Skin tissue was stained with hematoxylin eosin (H&E) for histological assessment, indicating non-necrotizing sarcoid granuloma. (C-K) Skin tissue was stained immunohistochemically using antibodies against the macrophage lineage marker CD68 (C,D), activated caspase-1 (E,F),or IL-1β (G,H). (I-K) Negative control stainings were obtained by applying respective isotype control antibodies. (L-O) Negative stainings obtained with the antigen-specific antibodies for skin from a healthy donor. The scale bar represents 500 μm in panels A,C,E,G and L,M,N,O, and 100 μm in panels B,D,F,H and I,J,K.*

Supplementary Figure S4

Figure S4: Western blot confirming active IL-1 released by sarcoid BAL cells. *Representative Western blot of an experiment in which supernatant of BAL cells derived from either sarcoid patients (SARK1 and SARK2) or from healthy volunteer (HV) were used. BAL cells were either unstimulated (ϕ) or stimulated with LPS for 4 hours and then stimulated w/wo ATP or nigericin (Nig) for further 2 hours. Western blot shows the production of the active, 17 kDalton form of IL-1β. The inactive 31 kaDalton pro-IL-1β form was much less released. Abbreviations: kDA: kilo Dalton, SARC: sarcoidosis, HV: healthy volunteer, Nig: nigericin.*

Supplementary Figure S5

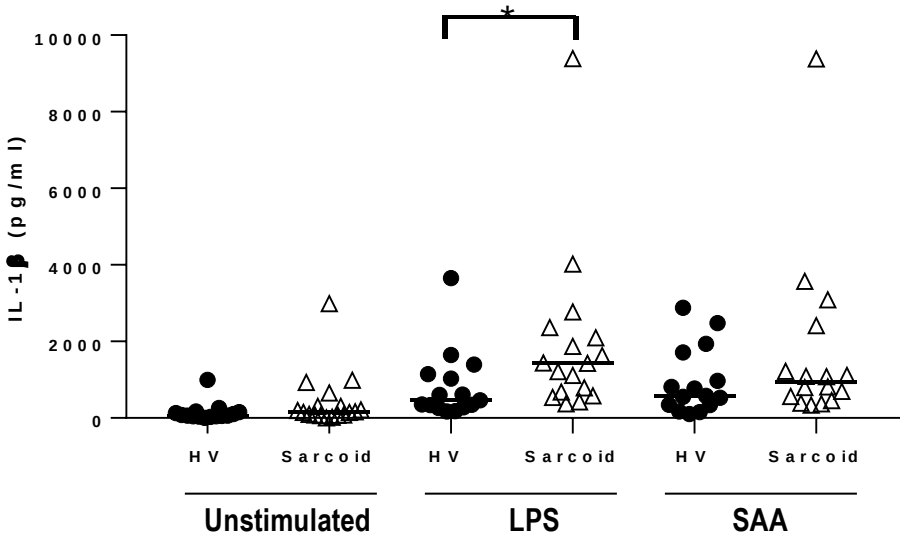

Figure S5: Significantly increased IL-1β production by sarcoid monocytes following LPS stimulation. *Monocytes were isolated from PBMCs of 19 sarcoid patients and 18 healthy volunteers (same study cohort as BAL cell experiments) and cultured for 4h w/wo stimulation with either LPS (1µg/ml) or SAA (1µg/ml). Following LPS but not SAA stimulation, sarcoid monocytes showed a significantly increased production of IL-1β (p=0.007) while in unstimulated monocytes there was a trend towards higher IL-1β production by sarcoid monocytes but comparison did not reach statistical significance (p=0.058). *p<0.05*

Supplementary Figure S6

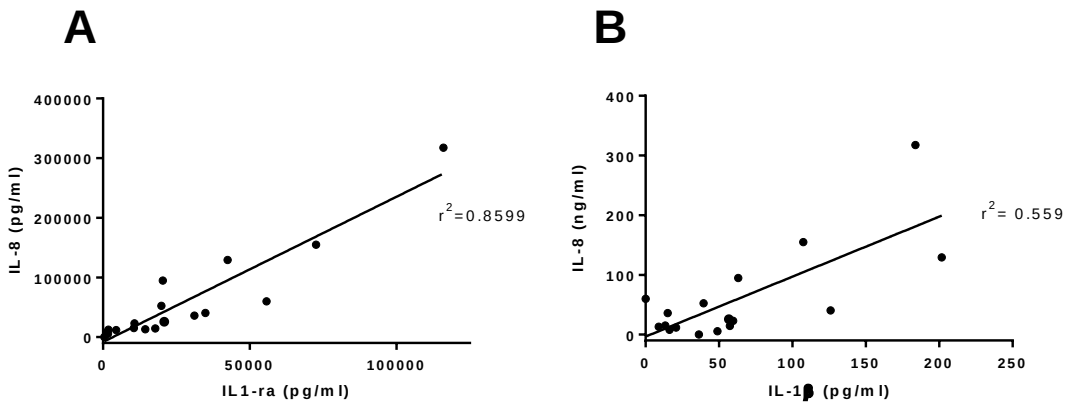

Figure S6: Close correlation of constitutive IL-1ra, IL-8 and IL-1β production levels of BAL cells from sarcoidosis patients. *(A) Significant correlation between IL-1ra and IL-8 production levels (r^2= 0.860, p<0.0001). (B) Significant correlation between IL-1β and IL-8 production levels (r^2= 0.559, p=0.0006).*

Supplementary Figure S7

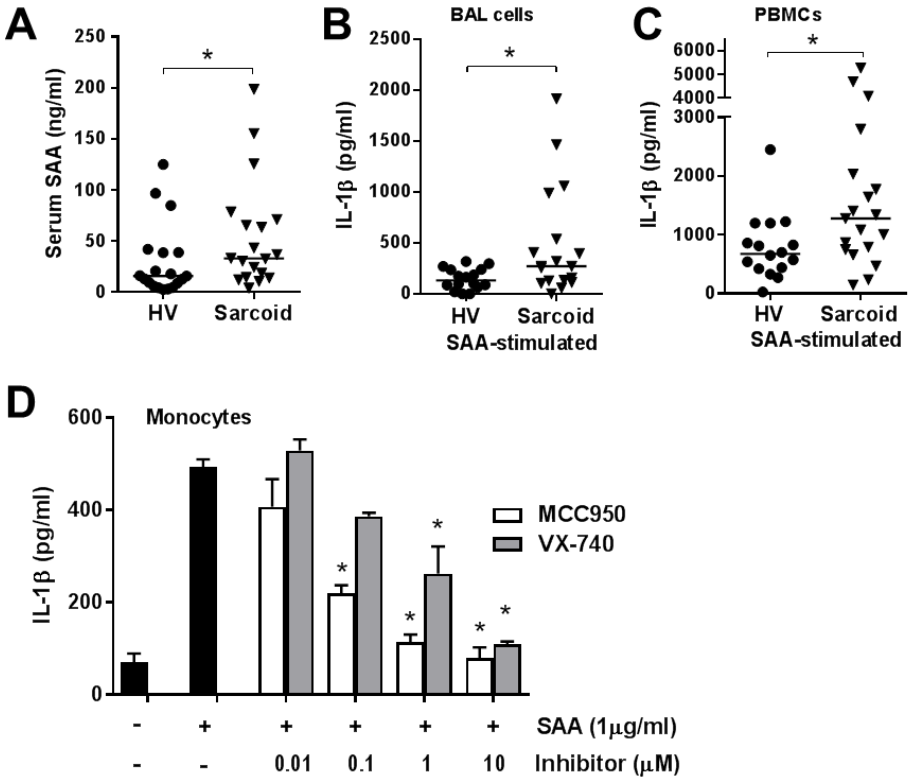

Figure S7: Higher SAA serum levels and responsiveness of BAL cells and PBMCs to ex vivo SAA stimulation in sarcoidosis. *(A) SAA levels measured in serum samples of HV (n=19) or patients with sarcoidosis (n=19). (B) BAL cells (HV n=16, SARC n=18) or (C) PBMCs (HV n=16, SARC n=19) from HV or sarcoid patients were stimulated with SAA for 24h and levels of IL-1β measured in the supernatants by homogenous time resolved fluorescence. The bars in panels A-C depict the median. *p<0.05, Mann-Whitney U test. (D) CD14 monocytes were isolated from the peripheral blood from healthy volunteers and stimulated with SAA for 24h with or without a caspase-1 inhibitor VX-740 or the NLRP3 inflammasome pathway inhibitor MCC950. IL-1β production following SAA stimulation was measured in the conditioned medium. The data indicate mean ± SEM from triplicate measurements of one out of 2 experiments with similar outcome. *p<0.05 for SAA-stimulated group w/wo compound treatment, ANOVA followed by Dunnett's multiple comparisons test.*

Supplementary Figure S8

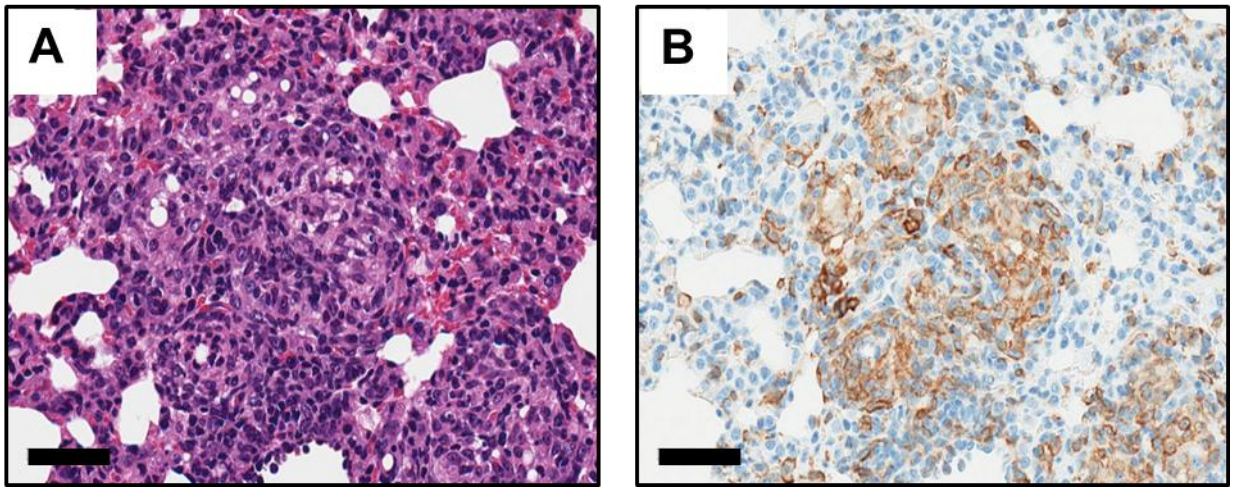

Figure S8. TDM induced pulmonary granuloma in mice resemble human sarcoid granuloma. *(A) High magnification of nonnecrotizing TDM-induced granuloma in lung of a WT mouse (hematoxylin and eosin stain). (B) Sections were stained by immunohistochemistry using antibodies against the macrophage lineage marker Iba-1. The scale bar represents 50 μm.*

Supplementary Figure S9

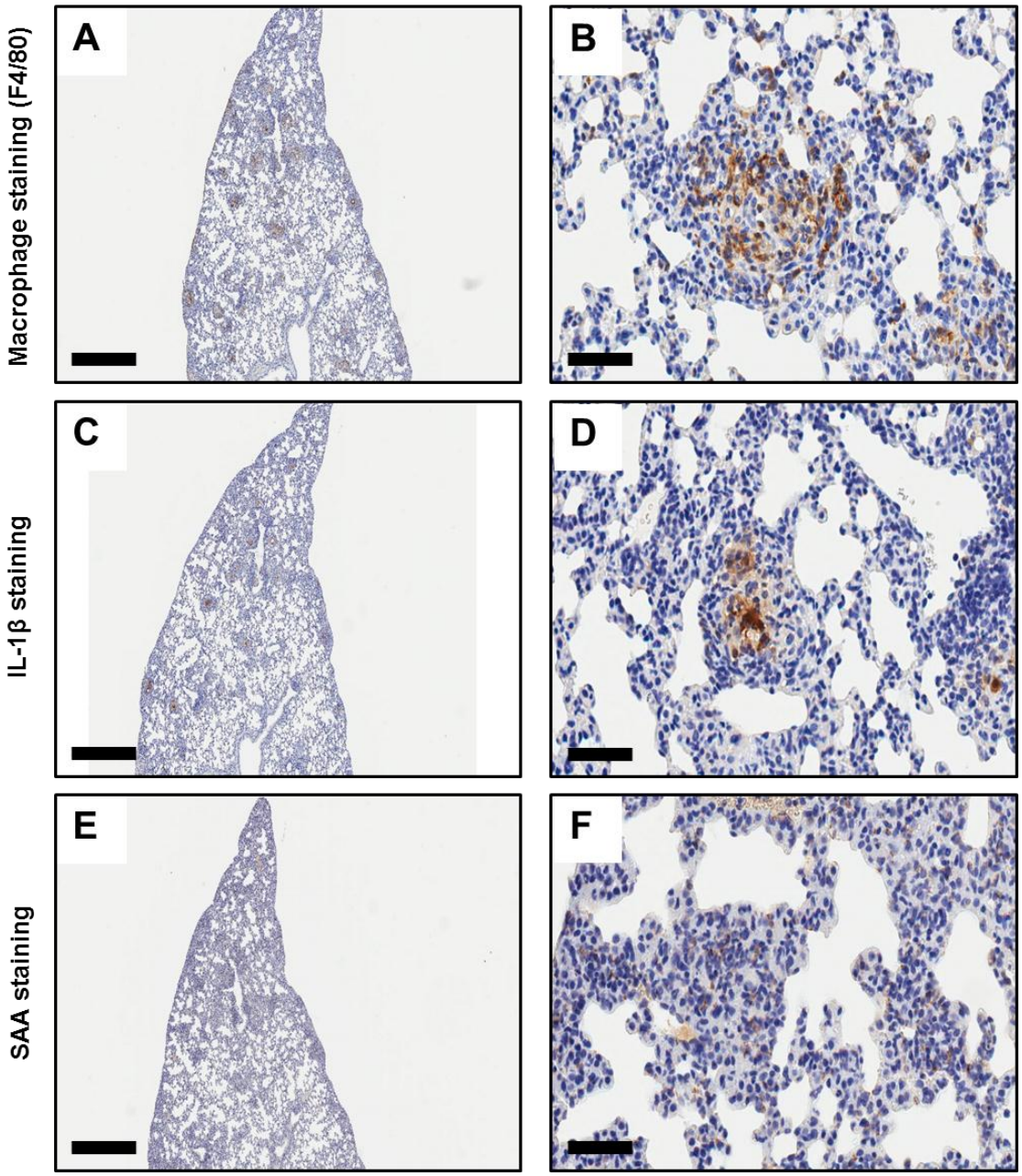

Figure S9. TDM induced pulmonary granuloma in mice consists of macrophages and express IL-1β and SAA. *(A,B) F4/80 staining demonstrates accumulation of macrophages in TDM-induced nonnecrotizing lung granuloma of WT mice. (C,D) IL-1β expression of presumably macrophages in the center of TDM-induced lung granuloma of WT mice. (E,F) SAA expression in the center of TDM-induced lung granuloma of WT mice. The scale bar represents 50 µm.*

Supplementary References

1. Prasse A, Katic C, Germann M, Buchwald A, Zissel G, Muller-Quernheim J. Phenotyping sarcoidosis from a pulmonary perspective. *Am J Respir Crit Care Med* 2008; **177**(3): 330-6.
2. Prasse A, Zissel G, Lutzen N, et al. Inhaled vasoactive intestinal peptide exerts immunoregulatory effects in sarcoidosis. *Am J Respir Crit Care Med* 2010; **182**(4): 540-8.
3. Prasse A, Pechkovsky DV, Toews GB, et al. A vicious circle of alveolar macrophages and fibroblasts perpetuates pulmonary fibrosis via CCL18. *Am J Respir Crit Care Med* 2006; **173**(7): 781-92.
4. Bauernfeind F, Rieger A, Schildberg FA, Knolle PA, Schmid-Burgk JL, Hornung V. NLRP3 inflammasome activity is negatively controlled by miR-223. *J Immunol* 2012; **189**(8): 4175-81.
5. Cornelis S, Kersse K, Festjens N, Lamkanfi M, Vandenabeele P. Inflammatory caspases: targets for novel therapies. *Curr Pharm Des* 2007; **13**(4): 367-85.
6. Mariathasan S, Weiss DS, Newton K, et al. Cryopyrin activates the inflammasome in response to toxins and ATP. *Nature* 2006; **440**(7081): 228-32.
7. Johnnidis JB, Harris MH, Wheeler RT, et al. Regulation of progenitor cell proliferation and granulocyte function by microRNA-223. *Nature* 2008; **451**(7182): 1125-9.
8. Yang G, Hisha H, Cui Y, et al. A new assay method for late CFU-S formation and long-term reconstituting activity using a small number of pluripotent hemopoietic stem cells. *Stem Cells* 2002; **20**(3): 241-8.
9. Schluns KS, Williams K, Ma A, Zheng XX, Lefrancois L. Cutting edge: requirement for IL-15 in the generation of primary and memory antigen-specific CD8 T cells. *J Immunol* 2002; **168**(10): 4827-31.
10. Janowska-Wieczorek A, Majka M, Kijowski J, et al. Platelet-derived microparticles bind to hematopoietic stem/progenitor cells and enhance their engraftment. *Blood* 2001; **98**(10): 3143-9.
11. Guidry TV, Hunter RL, Jr., Actor JK. Mycobacterial glycolipid trehalose 6,6'-dimycolate-induced hypersensitive granulomas: contribution of CD4+ lymphocytes. *Microbiology* 2007; **153**(Pt 10): 3360-9.
12. Perez RL, Roman J, Roser S, et al. Cytokine message and protein expression during lung granuloma formation and resolution induced by the mycobacterial cord factor trehalose-6,6'-dimycolate. *J Interferon Cytokine Res* 2000; **20**(9): 795-804.
13. Fejer G, Wegner MD, Gyory I, et al. Nontransformed, GM-CSF-dependent macrophage lines are a unique model to study tissue macrophage functions. *Proc Natl Acad Sci U S A* 2013; **110**(24): E2191-8.